2007

The Electroanalytical Performance of Sonogel Carbon Titanium (IV) Oxide Electrodes versus Conducting Polymer Electrodes in the Electrochemical Detection of Biological Molecules

Jelynn A. Stinson
Wright State University

The Electroanalytical Performance of Sonogel Carbon Titanium (IV) Oxide Electrodes versus Conducting Polymer Electrodes in the Electrochemical Detection of Biological Molecules

A thesis submitted in partial fulfillment of the requirements for the degree of Master of Science

BY

JELYNN ANNEULA STINSON
B.A., Wittenberg University, Springfield, Ohio, 1997
B.S., Wright State University, Dayton, Ohio, 2004

2007
Wright State University

WRIGHT STATE UNIVERSITY

SCHOOL OF GRADUATE STUDIES

May 30, 2007

I HEREBY RECOMMEND THAT THE THESIS PREPARED UNDER MY SUPERVISION BY Jelynn A. Stinson
ENTITLED The Electroanalytical Performance of Sonogel Carbon Titanium (IV)Oxide Electrodes versus Conducting Polymer Electrodes in the Electrochemical Detection of Biological Molecules
BE ACCEPTED IN PARTIAL FULFILLMENT OF THE REQUIREMENTS FOR THE DEGREE OF Master of Science.

_____
Suzanne Lunsford, Ph.D.
Thesis Director

_____
Kenneth Turnbull, Ph.D.
Department Chair

Committee on
Final Examination

_____
Suzanne Lunsford, Ph.D.

_____
David Dolson, Ph.D.

_____
Vladimir Katovic, Ph.D.

_____
Joseph F. Thomas, Jr., Ph.D.
Dean, School of Graduate Studies

ABSTRACT

Stinson, Jelynn Anneula. M.S., Department of Chemistry, Wright State University, 2007. The Electroanalytical Performance of Sonogel Carbon Titanium (IV) Oxide Electrodes versus Conducting Polymer Electrodes in the Electrochemical Detection of Biological Molecules.

The electrochemical performance of a newly developed sonogel carbon titanium (IV) oxide (SGC/TiO_2) electrode against poly(3-methylthiophene) (P3MT) and poly(2,2'-bithiophene) (PBTP) modified electrodes in the electrochemical detection of biological molecules is reported. The stability of the Titanium (IV) Oxide coating on the sonogel carbon electrode was shown to be greater than the P3MT coating on the conventional size glassy carbon electrode. After 10 consecutive scans, there was a 21% loss of the initial signal at the P3MT modified electrode and a 5% loss of the initial signal at the SGC/TiO_2 electrode.

The influence of NAD+ on NADH response was tested. The PBTP modified electrode and bare electrode demonstrated the inability to stabilize the interference due to NAD^+. The SGC/TiO_2 electrode was able to detour the susceptibility to interfering NAD^+. The response potential was improved by 141 mV. Response time for 5mM catechol (CAT) and 5mM ascorbic acid (AA) in 0.01M sulfuric acid was determined. Specificity for CAT detection was measured using a 5mM CAT + 5mM AA mixture in 0.01M sulfuric acid. The SGC/TiO_2 electrode permits a shorter response time and improved selectivity for CAT. NADH was irreversible in all electrolytes. Highest anodic peak potential, at the PBTP modified electrode, was measured in sodium nitrate. Highest anodic peak potential at the SGC/TiO_2 electrode was recorded in sulfuric acid.

TABLE OF CONTENTS

TABLE OF CONTENTS (cont'd)

TABLE OF CONTENTS (cont'd)

LIST OF TABLES

LIST OF FIGURES

LIST OF FIGURES (Con't.)

Figure Page

ACKNOWLEDGMENTS

The investigator wishes to express her sincere appreciation to Dr. Suzanne K. Lunsford for her assistance, guidance, and thoughts in pursuing this research. I would also like to thank Amber Yeary for her diligent work, as well as Brandon Van Ness for his technical support.

Special thanks are to be given to Dr. Dionysios D. Dionysiou and Dr. Hyeok Choi of the University of Cincinnati for their assistance in preparing and analyzing the sonogel carbon electrodes.

Lastly, I wish to thank the Lord Jesus Christ for blessing me with a wonderful and supportive family. To the Stinson and Brown family, I say thank you.

I. INTRODUCTION

Electroanalytical chemistry is a field of chemistry that uses analytical methods that are based upon oxidation/reduction reactions. It deals with oxidation/reduction reactions that are connected with the transfer of electric charge between a chemical species and an electrode. One of the most interesting aspects of electrochemistry is the homogenous chemical reactions that often accompany heterogenous electron-transfer processes occurring at the electrode –electrolyte interface. Electrodes used in electrochemical analysis are made up of a conductive metal. The charge that is transferred can be carried by an ion or an electron. The electrode surface that is in contact with the electrolyte solution acquires a charge and an electric potential that is different from bulk solution. Charge transfer takes place at the interface between the electrode and an electrolyte solution. The electrode surface acquires a charge when the electron is transferred between the metallic conductor, electrode, and the electrolyte solution. An electrode can be defined in both a broad sense and a narrower sense. In a broad sense the electrode can be viewed as an electrode system. It is defined as a system in which an ionically conductive phase, an electrolyte, is in contact with an electronically conductive phase, such as a metal or a semiconductor. In the narrower sense, the electrode would be defined as the metal or semiconductor that is dipped in the electrolyte solution. A diagram of the electrode system is shown in Figure 1.

The electrochemical reduction or oxidation of a dissolved molecule occurs at the electrode- solution interface. By placing a charged electrode in an electrolyte solution, the dissolved molecules are divided into two types: those that are in close proximity to

the electrode surface, able to take part in electrochemical reaction, and those that are a distance away from the electrode surface. Charged surfaces of the electrode in contact with electrolyte solutions attract ions of opposite charge and repel ions of like charge.

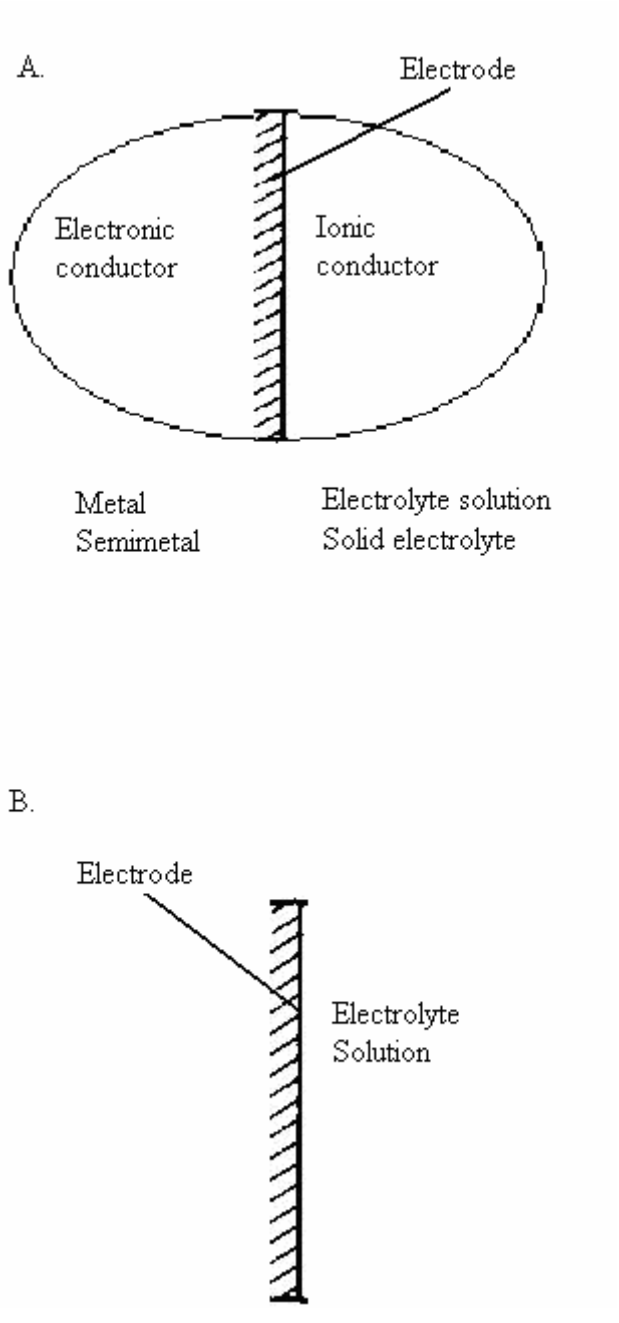

Figure 1: A) Electrode in a broad sense; B) Electrode in a narrower sense.

This repulsion and attraction establishes an "ion atmosphere" in the close proximity of the electrodes surface. [1] This ion atmosphere is composed of two parallel layers of charge. There is a layer of charge that is on the surface of the electrode itself and then there is a layer of oppositely charged ions near the surface. The interphase between the electrode and electrolyte solution has become known as the electrical double layer. [1] The interphase can act as a capacitor in its ability to store charge. As a result of this, Hemoltz proposed a parallel- plate capacitor model (Figure 2). This model was based on charge separation across a constant distance.

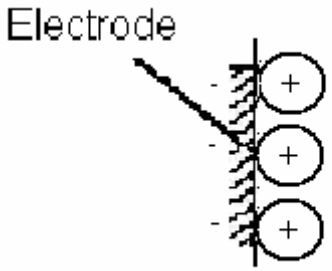

Figure 2. Simple capacitor model of the electrode-solution interphase.

The transfer of molecules from the bulk solution to the electrode surface must occur in order for electrochemical analysis to take place. This is referred to as mass transport. [1] Mass transport can be inhibited by other competing reactions that can occur at the electrodes surface. At this interface, there is interplay of mass transport with several phenomena. These phenomena include adsorption, chemisorption, and interfacial charge transfer. [1] The presence of all of these can make the interpretation of electrochemical data difficult. Solvent molecules that are not totally solvated have a tendency to absorb on the electrode surface. The absorption of these species can have a

profound affect on electrochemical experiments. Adsorption can alter electrode reactions, as well as virtually stop or enhance the rate of electron exchange. A common occurrence with absorption is the physical blocking of the electrode surface by the adsorbate. This forces a redox reactant to penetrate an absorbed film before exchanging electrons with the electrode causing distortion of the electrochemical signal. [1] The accumulation of an adsorbate at the electrodes surface has been used as a means of purposely modifying solid electrode surfaces.

Before the era of modified electrodes, clean inert surfaces were considered the ideal. Adsorption and polymerization were known to occur and known to influence electron transfer; however they were generally to be avoided. Interfacial phenomena often led to difficulties with solid electrode reproducibility and performance. There were strategies used by chemist to try and eliminate these interferences, only later were they exploited extensively and used in the study of modified electrodes. Modifying an electrode surface involves deliberately immobilizing a chemical on the surface of an electrode. By purposely absorbing and covalently attaching species to the surfaces of electrodes, the newly modified electrodes, display the chemical properties of the immobilized chemical. [2]

In 1975 R.W. Murray and L.L. Miller independently reported their first paper on modified electrodes. [3, 4] Initially research involved covalently bounding functional molecules on the electrode material in the form of monolayers. It was realized through further analysis that a modification of the electrode surface with a monolayer was insufficient. Electroactive polymeric films have a relatively higher number of active sites than the monolayered – modified surface. This makes the electrochemical process at the

polymer surface more pronounced. As a result of this, modification with polymer layers became increasingly popular. Electrons were shown to be shuttled from one site to the next through multilayered polymeric films, and finally to species in solution that were some distance from the electrodes surface. New theory was developed to explain this new electrode surface. In 1978 the first paper on polymer- modified electrodes was published by Miller and Van De Mark. [5]

Polymers helped to revolutionize electroanalytical techniques. Polymers offer versatility to the analytical chemists because of the wide range of reactions they can undergo. Conducting polymers have semi-conductive properties and can be switched between conducting and insulating states. Although conducting polymers are highly conductive, they require the addition or removal of electrons to obtain this high conductivity. The addition of electrons is called doping. The removal of electrons is called undoping. The doping and undoping mechanism for poly(3-methylthiophene) is shown in Figure 3.

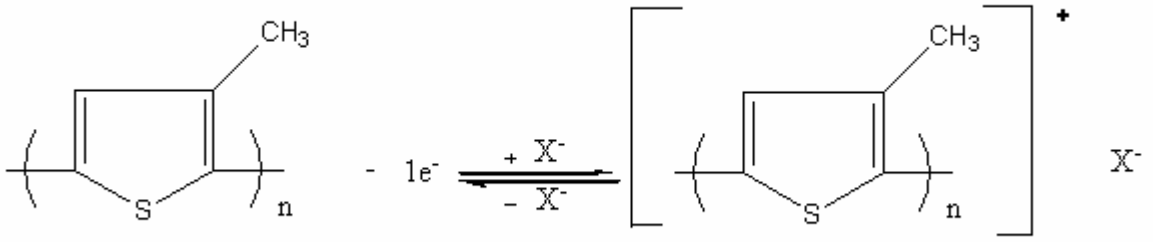

Figure 3**.** Doping and undoping mechanism for poly(3-methylthiophene).

Polymer morphology has a strong influence on charge transfer within the polymeric film. [6] The morphology of the polymer can be changed by changing the oxidation state of sites within the polymer. A dynamic change in the polymer occurs

during oxidation or reduction processes. The electrodeposition of a polymer film upon the surface of an electrode is initiated by the oxidation of a monomer to produce a radical cation. These radical cations present on the polymer backbone are called polarons/bipolarons. The polaron (1) and bipolaron (2) forms of polythiophene are shown in Figure 4.

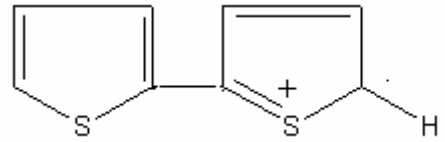

(1)

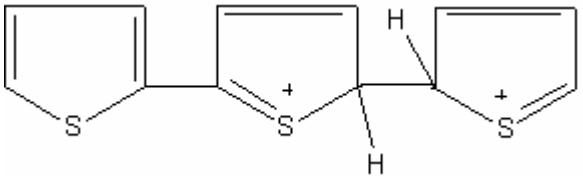

(2)

Figure 4. Polaron (1) and Bipolaron (2) forms of polythiophenes.

The free radical can combine with a second radical, or alternatively with neutral monomer molecule, to form a dimer. The dimer is accompanied by the loss of two protons. Oligomers are formed at the electrode surface during the initial steps of polymer deposition. These oligomers become the nucleation sites for further polymer elongation. As elongation progresses, and the film thickness increases, the film becomes increasingly amorphous. There is a high degree of inhomogeneity with conducting and insulating sites distributed throughout the film. [7] The morphology of polymer films is partially determined by the surrounding solution. The anions, which serve as dopants in the electropolymerization mix, stabilize the charged polaron/bipolaron. The rate of polymerization, stability of the polymer and conductivity, are all affected by the type of doping ion used during the electropolymerization process.

The electrolyte or solvent used in electroanalytical measurements can control charge transfer as well. The solvent used can be one that the newly deposited polymeric film interacts with favorably. When it favorably interacts, the film swells and become porous facilitating more transfer of electrons. On the other hand, the film can interact unfavorably in which case it can form a resistive layer that impedes penetration of electrons. There is a chance that the polymer films can become overoxidized. If overoxidation occurs, the polymers will undergo chain breakage and inter-chain repulsion. This would result in instability of the polymer matrix as well as loss of conductivity.

The main use of modified electrodes is electrocatalysis. Most work is centered on optimization of electrocatalytic processes. To enhance electrocatalysis it is best to increase the number of catalytic sites at the surface of the electrode. This accomplished by adsorption of a conducting polymer on the surface of an electrode. The thicknesses of the polymer layers as well as the permeability of ions help determine the efficiency of electrocatalysis. Linked with the development of modified electrodes is the use of ultramicroelectrodes (UME). UMEs have dimensions in the μm range. The advantage to using UMEs is enhanced mass transport, which leads to improved signal-to-noise ratios. At UMEs a smaller number of ions are needed to establish the double layer at a given potential, and also the iR drop due to uncompensated resistance is diminished. [9] Although polymer modified electrodes have helped to revolutionize electroanalytical techniques, they have not been widely used in practice of sensors because of instability, regeneration difficulties, irreproducibility of measurements, and often fragile films. To address the problems associated with the use of polymer modified electrodes, this present

research involves using the sol-gel method to develop a sonogel carbon electrode (SGC) modified with titanium (IV) oxide (SGC/TiO_2). Titanium (IV) Oxide is an inorganic pigment that is used in plastics applications that require outstanding resistance to heat, light, weathering, and solvents.

In this method a suspension of colloidal ceramic particles (sol) is converted to a gel by chemical treatment, and then dried and sintered to form a ceramic product. This process is generally used to develop nanoporous silica, titania or, organically-modified silica (ORMOSILS). [10] The steps involved in the sol-gel method are shown in Figure 5 for a Xerogel.

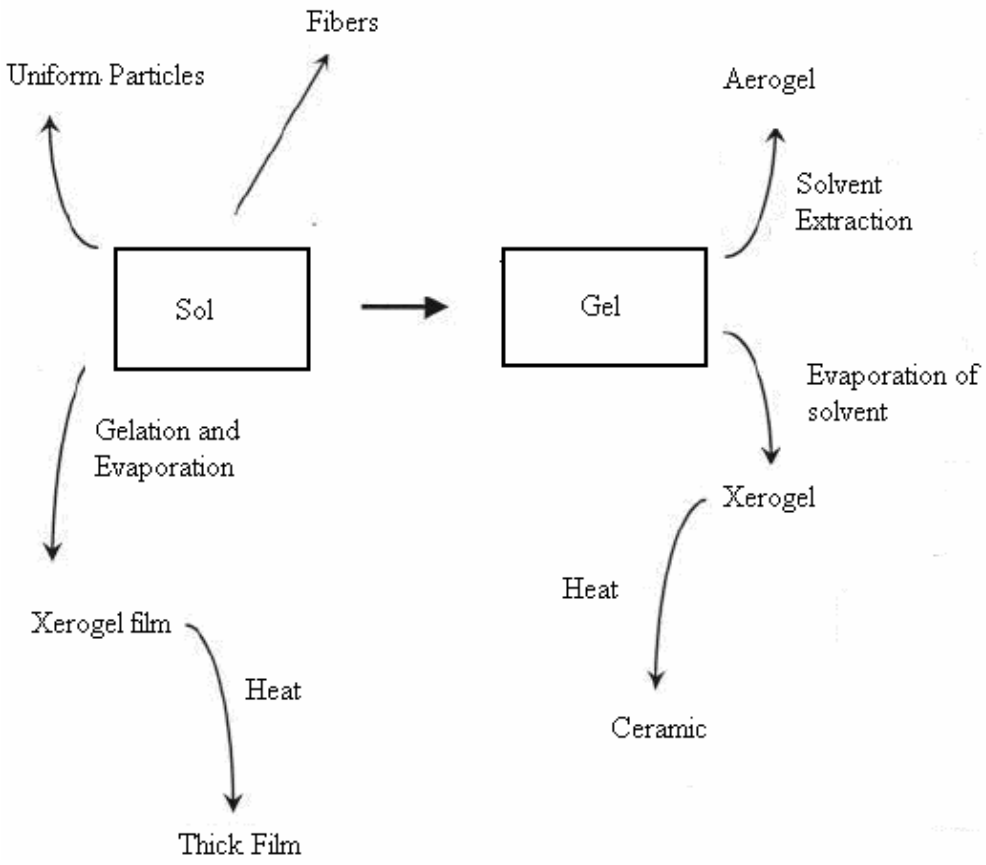

Figure 5. Description of sol-gel method. [10]

Typically tetraehoxysilane (TEOS) and tetramethoxysilane (TMOS) are used as silica precursors. Analyte sensitive reagents are added to the precursor and the nanoporous material acts as a support matrix. The nanoporous material encapsulates the analyte sensitive reagents in a cage-like structure. The support matrix works to immobilize the analyte sensitive material, so that it retains its stability and mobility over time. The analyte materials are usually added to the precursor solution, however it can be added in as a post-dopant. In this case, the analyte sensitive materials are added to a previously formed gel. This can be the most feasible method for gas sensors. Like polymers, the preparation of sol-gel is influenced by a number of parameters. The parameters that effect hydrolysis and condensation must be controlled, because of their influence on the final matrix of the nanoporous material. It is the matrix of the gel that controls the accessibility of the entrapped analyte sensitive material to the target analyte.

Although there is an interest in the use of these gels in analytical methods, historically these gels were being investigated for industrial use. [11] Early activity in sol-gel based sensors was directed mostly towards optical devices, because of the optical properties of silica .[12] Within recent years, the interest of employing the sol-gel method in the development of sensors has increased owing to the physico-chemical versatility of the process. [12] Along with versatility, they are easy to produce, undergo negligible swelling which allows ease of electron flow, as well as they exhibit increased mechanical stability. [12]

In the development of sensors, sensor stability, response time, and susceptibility to interfering species are critically important. This study demonstrates how the

SGC/TiO_2 electrode can be used as a sensor to detect samples of biological and environmental interest. This study evaluates the performance of a SGC/TiO_2 electrode against poly(3-methylthiophene) (P3MT) and poly(2,2-bithiophene) (PBTP) modified electrodes in the electrocatalytic detection of several samples of biological interest. The cyclic voltammetric behavior of dihydronicotinamide adenine dinucleotide (NADH)(1), catechol(CAT) (2) , and ascorbic acid (AA) (3) at a bare glassy carbon electrode(GCE), a PBTP modified GCE, P3MT modified GCE, and SGC/TiO_2 electrode is studied. The structures of the biological molecules studied are shown in Figure 6.

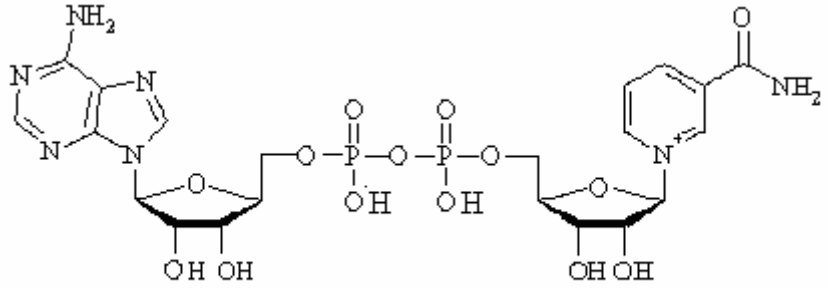

(1)

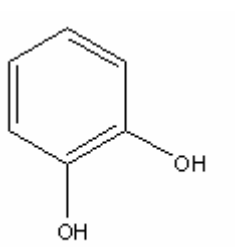

(2)

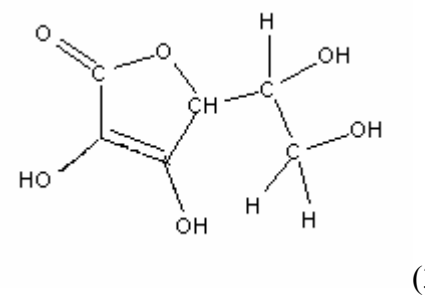

(3)

Figure 6. Structures of biological samples studied: NADH (1), CAT (2), and AA (3).

Cyclic voltammetry (CV) is a technique that has been used across many fields of chemistry to study redox states. It enables a wide potential range to be rapidly scanned for reducible or oxidizable species. It is thought to be the most versatile electroanalytical technique developed.[13] Its strengths are largely in diagnostic experimentation. It is useful

in the qualitative diagnosis of electrode reactions that are coupled to homogenous chemical reactions.

CV is a stationary-electrode voltammetric technique in which the potential applied across the double layer is scanned linearly from an initial potential to a final potential at a constant scan rate ν (mV/s). Stages within the scan in which the potential becomes increasingly positive is termed a positive scan.[1] Stages within the scan in which the potential becomes less positive is termed a negative scan. Generally scans are initiated at a potential at which no electrolysis occurs. By choosing the appropriate initial potential, unknown alterations in the reaction layer will not occur prior to beginning experimental applications.

The magnitudes of peak potential and the peak current are two important parameters in CV. Perhaps the biggest liability with using CV is the difficulty in obtaining accurate peak currents. An electrochemically reversible couple rapidly exchange electrons with the working electrode.[1] A reversible couple can be identified by using CV by measurement of the difference between the anodic and cathodic peak potentials. Electrochemical irreversibility is caused by slow electron exchange of the redox species with the working electrode and peak separations are dependent on scan rate.

One of the largest challenges of modern scientific research is to understand more about the function and morphology of the brain. Of high interest are the catecholamines and the NADH/NAD^+ coenzyme. Catecholamines are a class of neurotransmitters (1,2-dihydroxybenzenes) that are involved in a wide variety of physiological processes. [13] These classes of neurotransmitters are secreted in the brain and altered levels have been

associated with mental and behavioral disorders such as schizophrenia, attention deficient disorder, Alzheimer's disease, Parkinson's disease, eating disorders, epilepsy, amphetamine addiction, and cocaine addiction. [14] Voltammetric detection of catecholamines is effected by the presence of interferents such as ascorbic acid. The concentration of ascorbic acid (AA) varies from species to species. AA concentration range from 1.0×10^{-7} to $1.0\times10^{-3} M$. [14]

$NADH/NAD^+$ redox coenzymes are of extreme importance in biological systems. There is a reducing potential that is stored in NADH that can be converted to adenosine triphosphate (ATP). ATP "energy" is necessary for an organism to live. Therefore the development of a biosensor for its detection is of great interest for analytical purposes. The detection of NADH has been the focus of many studies. [15-20] The electrochemical detection of NADH is often plagued by interferences that come from products of side reactions, as well as the adsorption of NAD^+ .[16] Previous research has shown that the selectivity of NADH in the presence of such interferences may be difficult. Also the detection of NADH requires high applied potentials and is highly irreversible.

There are challenges encountered in the analysis of clinical and environmental samples because their detection is effected and accompanied by the presence of interferents. These challenges can be addressed by improving the stability, rigidity, and electrocatalytic properties of the electrode. This research will demonstrate how the electron transfer ability of the newly developed sonogel-carbon electrode is dramatically improved in comparison to a bare glassy carbon electrode (GCE), as well as demonstrate its improved stability and enhanced electrocatalytic properties against that of a poly(3-methylthiophene) (P3MT) and poly(2,2-bithiophene) (PBTP) modified electrode.

II. EXPERIMENTAL

Polymer Modified Electrodes

Chemicals

Acetonitrile (HPLC grade), tetrabutylammonium tetrafluoroborate(TBATFB), sulfuric acid (A.C.S. Reagent), 2,2'-bithiophene and 3-methythiophene were all obtained from Aldrich Chemical Company. The 0.005 M 3-methylthiophene and 0.005 M 2,2'-bithiophene solutions were prepared freshly in 0.1 M TBATFB dissolved in acetonitrile (ACN) solution.

Surface Preparation

Before electropolymerization the working glassy carbon electrode (MF-2012, BAS) was polished on nylon cloth using 2 micrometer diamond paste first then polished on microcloth using 0.05 micrometer Alumina (CF-1050, BASi). The glassy carbon electrode (MF-2012,BAS., Inc., West Lafayette, IN USA) was rinsed with HPLC grade acetonitrile and air dried for approximately 15 minutes. The electropolymerization of the 3-methylthiophene and the 2,2'bithiophene at a polished glassy carbon electrode was carried out in a single compartment cell as illustrated in Figure 6.

A platinum (Pt) wire was the auxillary electrode (120 mm long, 0.3 mm diameter wire) and the reference electrode was an Ag/AgCl/3M NaCl (MF-2074, BAS) placed in the compartment cell. The polymerization of the new modified electrode surfaces was carried out by cyclic voltammetry. Both the polymerization of the 3-methylthiophene and 2,2-bithiophene was performed on a PAR 175 Potentiostat-Galvanostat. The polymerization of 2,2'-bithiophene and 3- methylthiophene was done using cyclic sweep technique. For 2,2-bithiophene, films were grown by cyclic sweep from 0 to 1000 mV

for 6 cycles, Figure 7. For 3- methylthiophene, films were grown in three different potential ranges: 0 to 1500 mV; 0 to 1650 mV; and 0 to 1800 mV. The electrode was swept for one cyclic cycle in each range, Figure 8. The scan rate for both electropolymerizations was 100 mV/s. Both the P3MT and PBTP electrodes were rinsed with acetonitrile and then immersed in a monomer free TBATFB solution. The modified electrodes were scanned from 0 to 1800 mV to undope the electrolyte anion.

Hazards

The hazards associated with this experiment were mainly due to the corrosive nature of sulfuric acid and toxicity of monomers. Therefore all work was performed under a ventilation hood while wearing protective garments such as a laboratory coat, safety goggles and gloves.

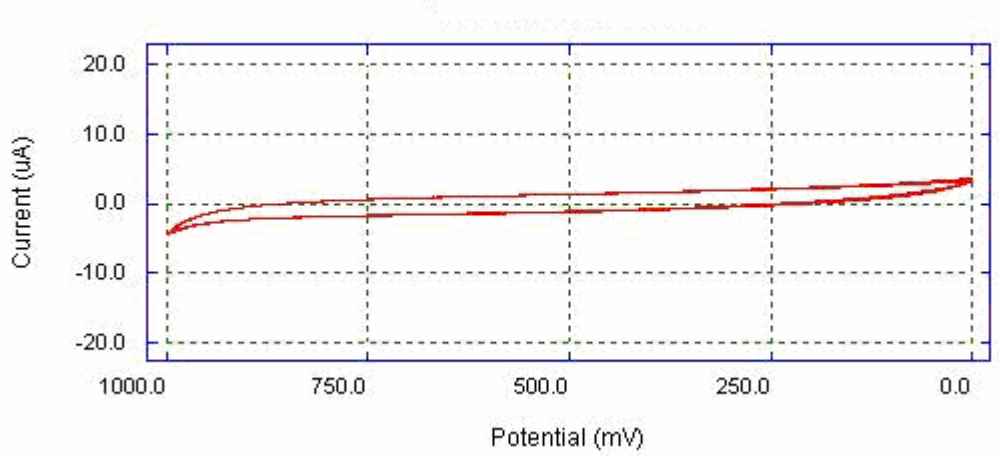

Figure 7. Poly(2,2'-bithiophene) (PBTP)Glassy Carbon Electrode(GCE) Preparation. Cyclic Voltammogram (CV) of 5mM 2,2'-bithiophene in 0.1 M tetrabutylammoniumtetrafluoroborate/acetonitrile (TBATFB/ACN) Scan Rate = 100 mV/s.

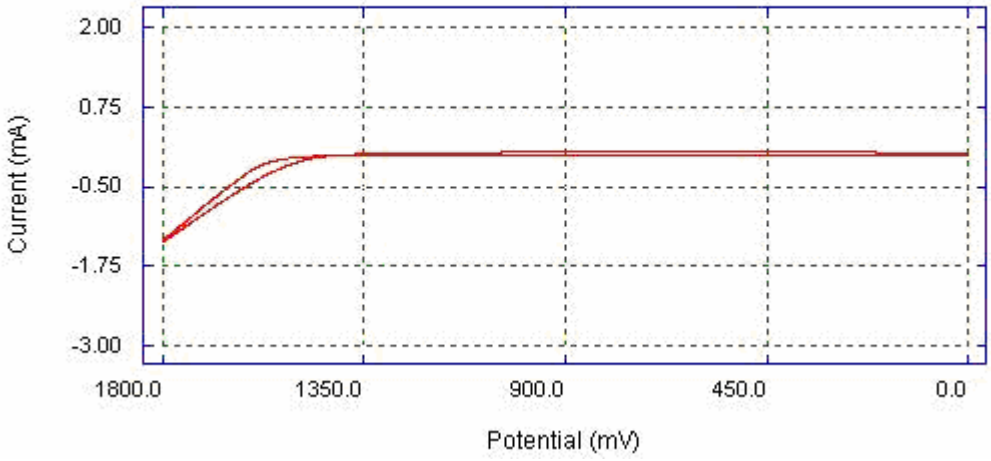

Figure 8. Poly(3-methylthiophene) (P3MT) GCE preparation applied potential range 0 to1800 mV. CV of 5mM 3-methylthiophene in 0.1M TBATFB/ACN. Scan Rate = 100 mV/s.

Characterization of Polymer modified Surfaces

The electrode surfaces of the PBTP modified electrode was investigated at the micro-level using a JEOL 35 Scanning Electron Microscope (SEM).

Sonogel Carbon Electrode/TiO_2 (SGC/TiO_2)

Making the Sonogel Carbon Electrode (SGC)

1.5 ml of methyltrimethoxysilane (MTMOS, Fluka) was added into 0.3 ml of 0.2 M HCl solution. This mixture was sonicated in an ultrasonicator (2510R-DH, Bransonic) for 15 s. Following sonication, 3 g of graphite carbon powder (Alfa Aesar, 99.999%) was added into the MTMOS solution and mixed thoroughly for 10 min, where the total volume of the reactants was significantly reduced up to 20%, condensing the SGC. A 0.25 mm copper wire (Alfa Aesar) was installed inside a 0.69 mm I.D. capillary glass tube (Sutter Instrument) used as the bodies of the SGC electrode. The glass tube

was filled with the SGC, and dried at 40◦ C for 24 h. The tip of the SGC electrode was polished with a fine sand paper, and then wiped with a soft tissue.

Modification of SGC with nanostructured TiO_2

Preparation of TiO_2 sol-gel

Polyoxyethylenesorbitan monoleate (Tween 80, Aldrich) surfactant was selected as a pore directing agent in TiO_2 sol. A suitable amount of Tween 80 was homogeneously dissolved in isopropanol (iPrOH, Fisher). Acetic acid (Fisher) was added into the solution for the esterification reaction with iPrOH to generate water .[23] Titanium tetraisopropoxide (TTIP, Aldrich) was added to the solution as a TiO_2 precursor. Hydrolysis and condensation reactions of TTIP occurred, forming a stable TiO_2 sol. The molar ratio of the ingredients was optimized at Tween 80: iPrOH: acetic acid: TTIP = 1:45:6:1.

SGC Coating

The tip of the SGC electrode was coated by dipping it into the TiO_2 sol for 3 s and removing it. After coating, the SGC/TiO_2 electrode was dried at room temperature for 1 hour and calcined in a multi-segment programmable furnace (Paragon HT-22-D, Thermcraft) to remove the surfactant templates and obtain a desirable crystal phase of TiO_2. Furnace temperature was increased at a ramp rate of $3^{\circ}C\ min^{-1}$ to 500° C, maintained at this temperature for 20 min, and cooled down naturally.

Characterization of SGC/TiO_2

It was difficult to characterize the properties of TiO_2 materials on the SGC electrode. Due to the difficulty, easy to remove TiO_2 coating was prepared on borosilicate glass (Micro slide, Gold Seal), assuming that if the substrate changes, the

porous structure and crystal phase of TiO_2 are similar since those properties originate from the surfactant addition and heat treatment rather than the substrate properties [24]. X-ray diffraction (XRD) analysis, using a Kristalloflex D500 diffractometer (Siemens) with Cu Kα (λ= 1.5406 Å), was used to determine the crystallographic structure of TiO_2. Along with X- ray diffraction, a porosimetry analyzer (Tristar 3000, Micromeritics) was used to determine the Brunauer, Emmett, and Teller (BET) specific area, porosity, and pore size distribution in the mesoporous range of TiO_2. The structure of TiO_2 materials at the nano-level was visualized using a JEM-2010F (JEOL) high resolution-transmission electron microscope (HR-TEM) with a field emission gun at 200kV. TiO_2 sample was scratched from the easy-to-remove TiO_2 coating on glass substrate and dispersed in methanol and fixed on a carbon-coated copper grid (LC200-Cu, Electron Microscopy Sciences). The electrode surface of the SGC/TiO_2 was investigated at the micro-level using an environmental scanning electron microscope (ESEM, Philips XL 30 ESEM-FEG). Connected to the HR-TEM and ESEM was an energy dispersive X-ray spectroscope (EDAX, Oxford Isis) used to analyze the elemental composition of TiO_2.

Cyclic Voltammetry Studies

Electrochemical measurements were carried out with an Electrochemical Workstation (Epsilon, Bioanalytical Systems), based on cyclic voltammetry (CV) employing three electrodes: Pt auxiliary electrode (Bioanalytical Systems), Ag/AgCl reference electrode (Bioanalytical Systems), and SGC/TiO_2 along with bare and polymer modified GCEs served as working electrodes. To investigate the performance of the SGC/ TiO_2 against bare GCE and polymer modified GCEs, samples of interest were prepared as follows: Catechol (Fluka) of 5mM solution was prepared in 10mM sulfuric

acid (Aldrich) pH 1.7; ascorbic acid (Aldrich) of 5mM solution was prepared in 10mM sulfuric acid (Aldrich) pH 1.7; NADH (Sigma Aldrich) of 5mM solution was prepared in several electrolytes. These electrolytes included: 0.1 M phosphate buffer with 0.1M NaCl at pH of 6.82; 0.1M sodium nitrate (Fisher Scientific); 0.1M nitric acid (Aldrich); 0.1M sulfuric acid (Aldrich); 0.1M sodium sulfate (Fisher). For testing influence of scan rate effects on NADH peak current, scan rates utilized were 25 mV/s; 50 mV/s; 75 mV/s; 100 mV/s. These were taken in phosphate buffer solution.

In a practical lode, an electrochemist does not always know either the standard redox potential or redox state for species in solution. One generally wants to use an initial potential scan at an initial potential (E_i) at which no electrolysis occurs. In this study, redox potentials for the analyte molecules were determined by trial and error. Potentials were determined by observing the absence or prescence of faradaic current occurence. The scan rate for catechol and ascorbic acid detection was 100 mV/s. The scan rate for NADH detection was 50 mV/s. The chemical bonding between TiO_2 and catechol during the experiment was monitored using Fourier transform infrared spectroscope (FTIR, Perkin-Elmer 1610), by measuring absorption changes. To investigate the relation between current in CV and catechol concentration, catechol concentration was varied between 0.1 and 1.0 mM.

III. RESULTS AND DISCUSSION

Introduction

Issues of sensor stability, response time and/or specificity and susceptibility to interfering species are critically important in evaluating sensor performance and potential for commercial development. In the present study efforts were directed toward examination of the SGC/TiO_2 electrodes use as a sensor in the detection of NADH, CAT, and AA against electroanalytical techniques developed and used by previous workers in studies involving the electropolymerization of electrode surfaces with conductive polymers. [1]

A discussion of the SGC/TiO_2 electrode properties will be followed by a comparison of the SGC/TiO_2 electrode stability, response time, and specificity of response to a PBTP and P3MT modified electrode.

Structural Characteristics of TiO_2 particles

Structural properties of TiO_2 were investigated by using powder collected from the easy-to-remove TiO_2 on glass substrate. The collected powder was analyzed by using HR-TEM and porosimetry analyzer. Figure 9, the HR-TEM image of TiO_2, shows the morphology of the nanostructured TiO_2. The TiO_2 was highly porous and had a distinct pore structure with an average diameter of 5nm. Films were composed of highly interconnected networks, which indicated the Tween 80 used in the synthesis of the films effectively acted as a pore directing agent. [26,29] The accessibility of the reactants to or from the active sites in TiO_2 is contingent upon the mesoporous structure of the film. [30] Pore sizes ranged from 2 to 8 nm. The porous structure was reported to exhibit high adsorption ability for the reactants, in this case catechol, following enhanced reaction. [30]

XRD analysis showed that the TiO_2 heat-treated at 500 ˚C is active anatase crystal phase with crystallite size of approximately 9nm.

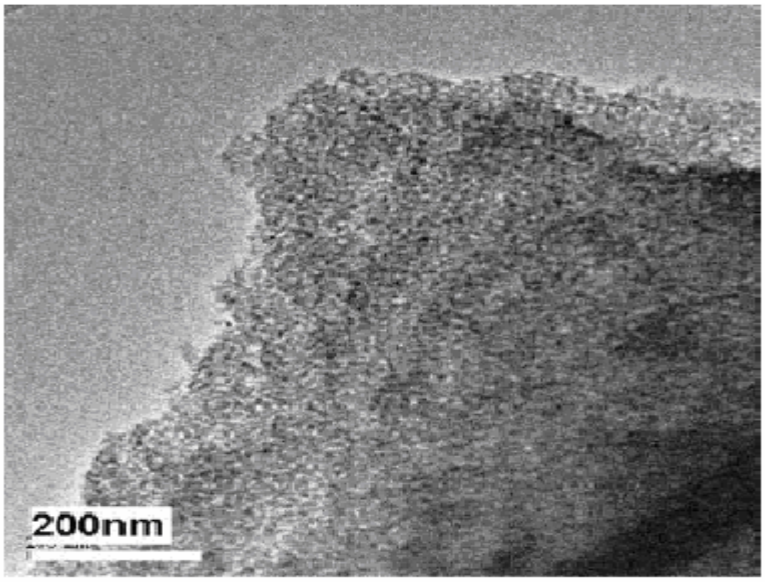

Figure 9. HR- TEM image of TiO_2 particles taken from the SGC/TiO_2 electrode.

Figure 10 shows the ESEM images of a PBTP tip (a) and a SGC/TiO_2 tip (b). The tip of the electrode was packed well with graphite powder. As Figure 10 shows, there were no serious micro-cracks and defects in the structure of the synthesized TiO_2 film upon the SGC tip surface. The uniformity by which the TiO_2 coats the electrode tip is not observed for the PBTP modified tip. To further support conclusion of TiO_2 uniformity, EDAX analysis taken at various spots on the SGC tip showed similar elemental composition. Values in Table 1 represent the EDAX elemental composition at the SGC/TiO_2 tip. As is shown carbon, silicon, titanium, and oxygen were identified as major elements. Respectively, their sources were graphite powder, MTMOS, TTIP, oxides, and surface hydroxyl groups.

Table 1

EDAX elemental composition at the tip of the SGC/TiO_2 electrode

Element	Wt %	At %
Carbon, C	78.05	86.37
Oxygen, O	13.14	10.92
Silicon, Si	01.38	00.65
Titanium, Ti	07.43	02.06

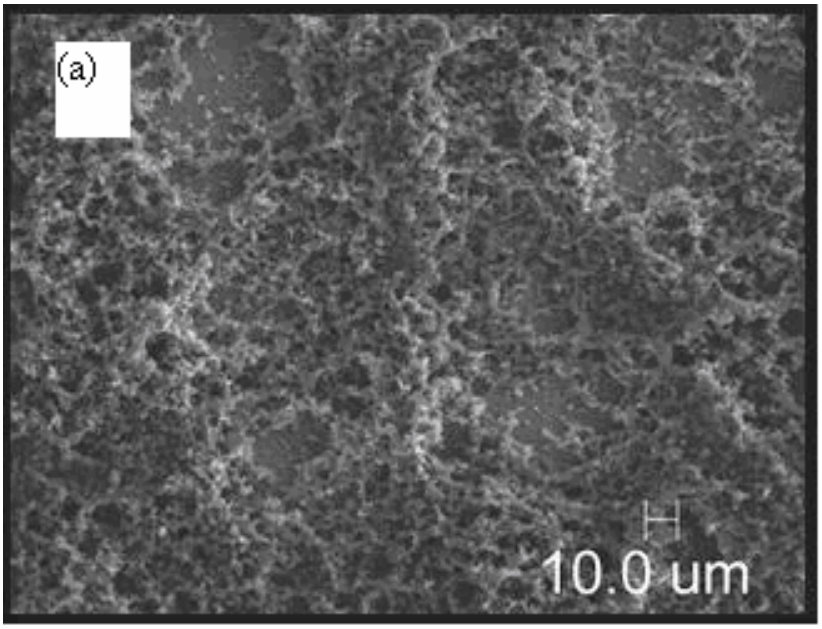

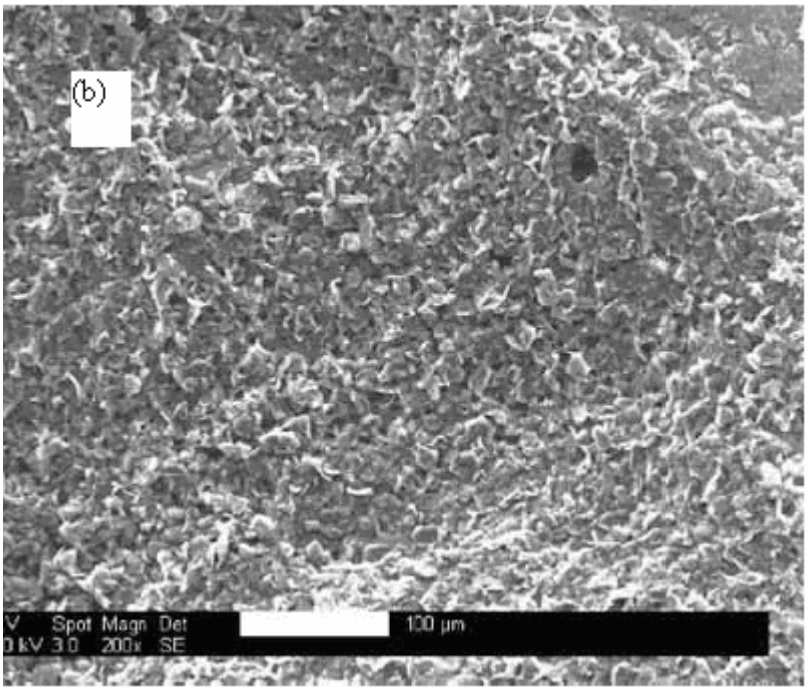

Figure 10**.** (a) SEM image of PBTP modified electrode tip (scale bar = 10.0 µm) and (b) ESEM image of SGC/TiO_2 electrode tip (scale bar = 100 µm).

Detection route and mechanisms for CAT

Important IR peak designations are summarized in Table 2. Values are compared with findings by Martin et al. [31] Main bands and assignments are as follows: 1491 cm^{-1}, stretching (C-C);1451 cm^{-1}, stretching (C=); 1258cm^{-1}, stretching (C-O); 1208 and 1095 cm^{-1}, bending (C-H). The 1198 cm^{-1} –OH wag is absent for the doubly deprotonated species and the 1353 cm^{-1} in-plane –OH bending is not seen (only a weak and broad feature centered at 1208 cm^{-1} was seen). From the designated/assigned IR values a possible mechanism for the detection of CAT at a SGC/TiO_2 electrode is suggested to follow the scheme shown in Figure 11. [32] The TiO_2 accelerates the transfer of electrons between the SGC and CAT. CAT absorbed onto TiO_2 rapidly reaches the SGC surface, and then is oxidized, involving two electrons (e^-) and two protons (H^+). Similar observations on enhanced absorption and acceleration of proton transfer step were reported. [33,34] The surface of TiO_2 acts as a redox mediator for the electron transfer between the SGC electrode and CAT. [35,36]

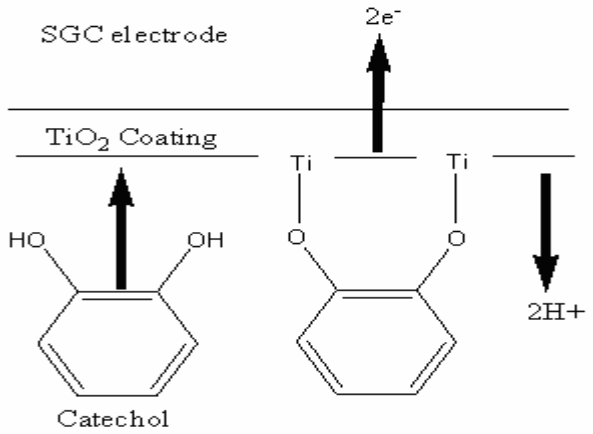

Figure 11. Bonding and electron transfer scheme between catechol and the SGC/TiO_2 electrode.

Table 2

Infra-Red bonding assignments between Titanium (IV) Oxide and catechol at pH 7.0[a]

Frequencies (cm^{-1})		Assignments
Catechol + TiO_2 [Ref. 30]	Catechol adsorbed on nano-structure TiO_2 in this study	
1068	1058	γC-H in plane
1486	1491	ν (C-C-)
1450	1451	ν(-C=C-)
1263	1258	ν (C-O)
1215; 1105	1208;1095	γ (C-H) in plane

[a] This test was performed with nanostructure TiO_2 thin film immobilized on glass substrate.

Calibration Curve

To quantitatively analyze CAT at a low concentration using the SGC/TiO_2 electrode, concentrations of CAT was varied within a range from 0 to 1.0 mM. The difference in reduction current (I_{pc}) and oxidation current (I_{pa}), ΔI, was followed using cyclic voltammetry and presented in Eq. (1).

$$\text{CAT concentration (mM)} = 47.62 \times (I_{pc}(\text{mA}) - I_{pa}(\text{mA})) \quad (1)$$

As Figure 12 shows, the linear relation between ΔI and CAT concentration was observed with $R^2 = 0.988$. Result implies that the SGC/TiO_2 can detect CAT quantitatively.

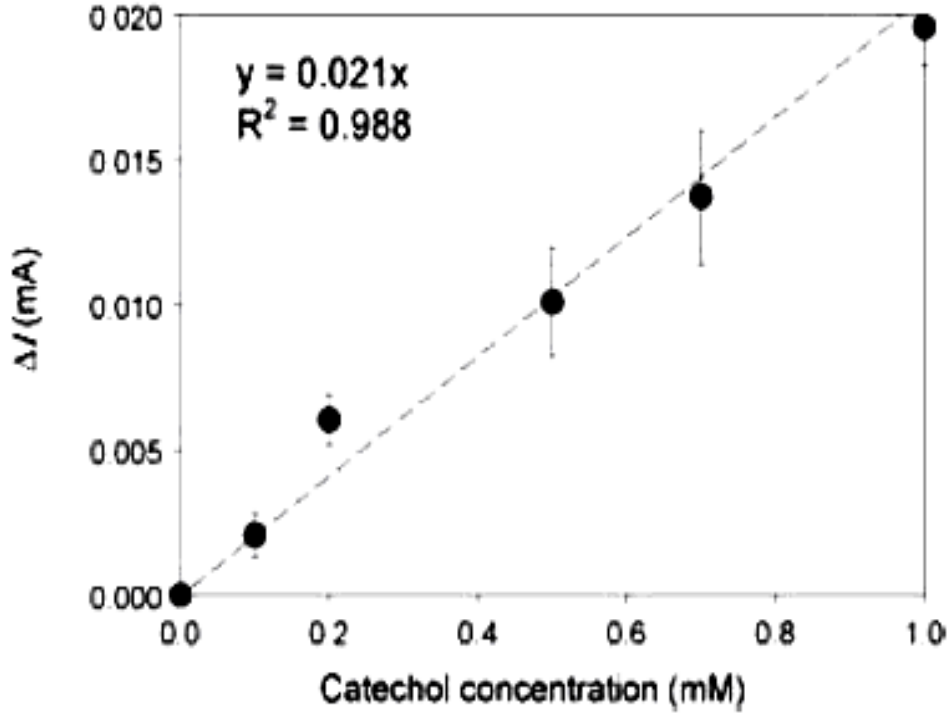

Figure 12. Calibration curve showing the relation between cyclic voltammetry current and catechol concentration. Error bars indicate standard deviation of cyclic voltammetry result.

Response Time

In chemical sensor applications the time duration required to achieve a useful response is an important feature. Response time can be the critical performance factor in situations such as medical conditions and industrial process monitoring. Response time is influenced by a number of factors. Those of interest to this study include number of electrons involved in the overall electron transfer reactions taking place at the electrode surface as well as diffusion time through the matrix of the immobilized chemical on the electrodes tip. Like the SGC/TiO_2 electrode, the P3MT modified GCE has indicated the reversibility of CAT oxidation significantly improved compared with the bare GCE.

Voltages applied during electropolymerization were varied and the response times at the modified electrode surfaces varied with applied voltage. The cyclic voltammograms for P3MT modified GCEs prepared by applying 1800 mV, 1650 mV, and 1500 mV in the detection of CAT are shown in Figures 14, 15**,** and 16. The applied voltage that presented the most optimum conditions for electrochemical analysis of CAT and AA was 1800 mV. Peak potential difference between anodic and cathodic peaks, ΔE, was 84 mV at the SGC/TiO_2 electrode (Figure 13) and 191 mV at the 1800 mV P3MT modified GCE. In buffer solution, pH of 6.82, ΔE was 59 mV at the SGC/TiO_2 electrode. CAT exhibited reversible electron transfer behavior at the SGC/TiO_2 electrode. The values of anodic peak current (i_a) and cathodic peak current (i_c) are similar in magnitude for a reversible couple with no kinetic complications. This is quantitatively described by the following equation:

$$\frac{i_a}{i_c} \approx 1$$

Peak current ratio values deviation from 1 illustrate the influence by chemical reactions coupled to electrode processes that effect kinetic behavior. Peak current ratio values are shown in Table 3. As proposed by the data, the SGC/TiO_2 electrode exhibited enhanced reversibility in comparison to the P3MT modified GCEs in the electroanalytical detection of CAT. There are well defined oxidation and reduction responses at the SGC/TiO_2 electrode.

It appears that the electron transfer involved in CAT electrochemical detection is quasi-reversible at the P3MT modified GCEs grown by scanning 0 to 1500mV and 0 to 1600 mV. When the electron transfer reaction is quasi-reversible the rate of electron transfer is too slow to keep the redox couple in equilibrium when the potential is changed

rapidly. Consequently, the recorded voltammograms deviate from the ideal shape. In particular, when the rate of electron transfer is sluggish, ΔE is greater. AA exhibited irreversible electron transfer behavior at both the SGC/TiO_2 electrode and P3MT modified GCE.

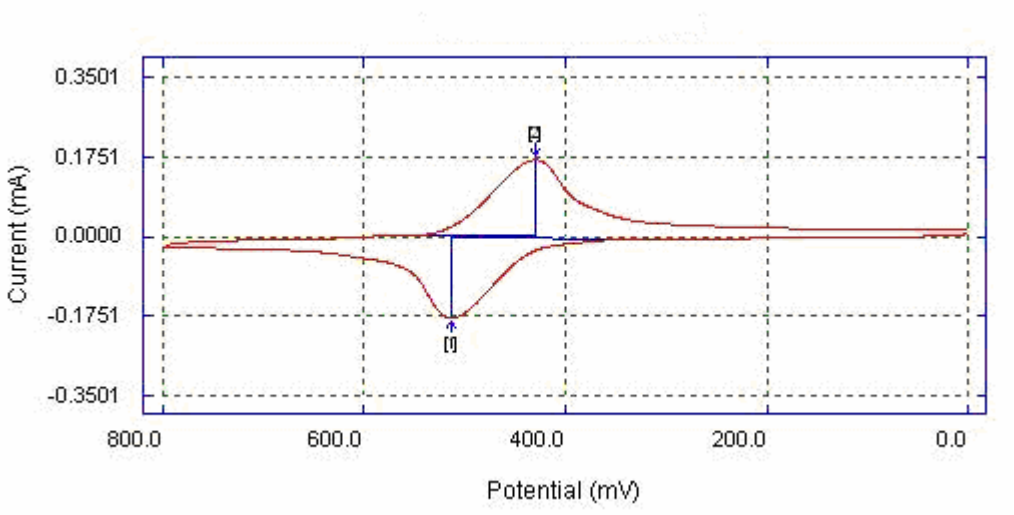

Figure 13. Cyclic voltammogram of 5mM CAT in 0.01 M sulfuric acid at a SGC/TiO_2 electrode. Scan rate = 100 mV/s.

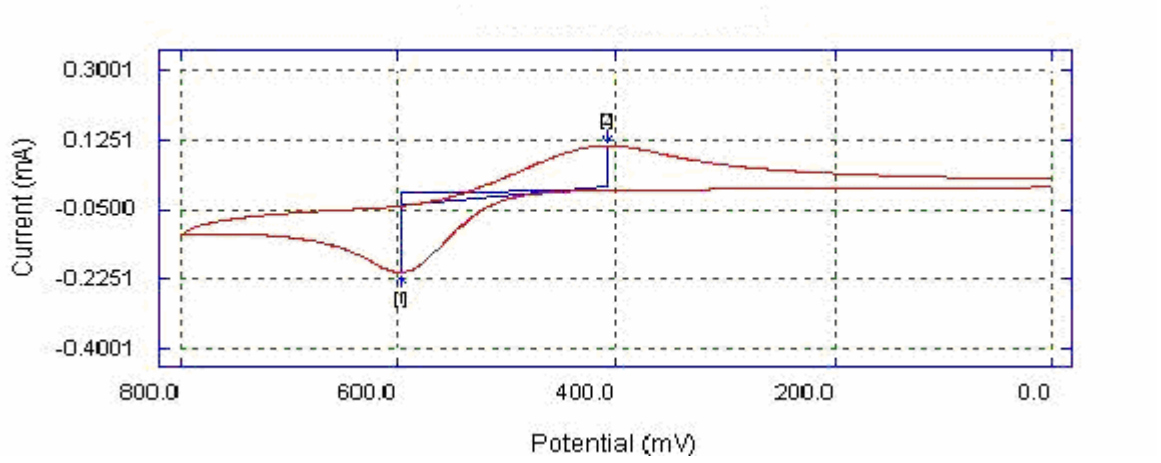

Figure 14. Cyclic voltammogram of 5mM CAT in 0.01 M sulfuric acid at a P3MT GCE grown 1800 mV. Scan rate = 100 mV/s.

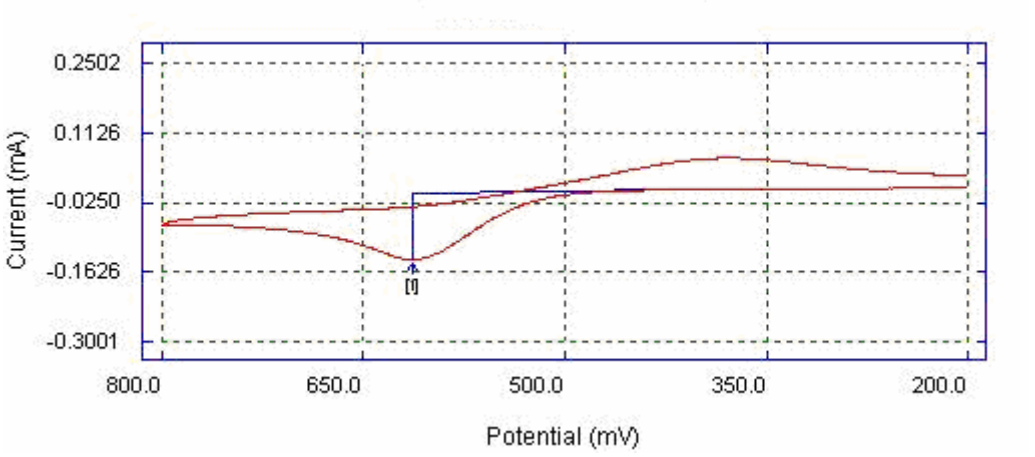

Figure 15. Cyclic voltammogram of 5mM CAT in 0.01 M sulfuric acid at a P3MT GCE grown 1650 mV. Scan rate = 100 mV/s.

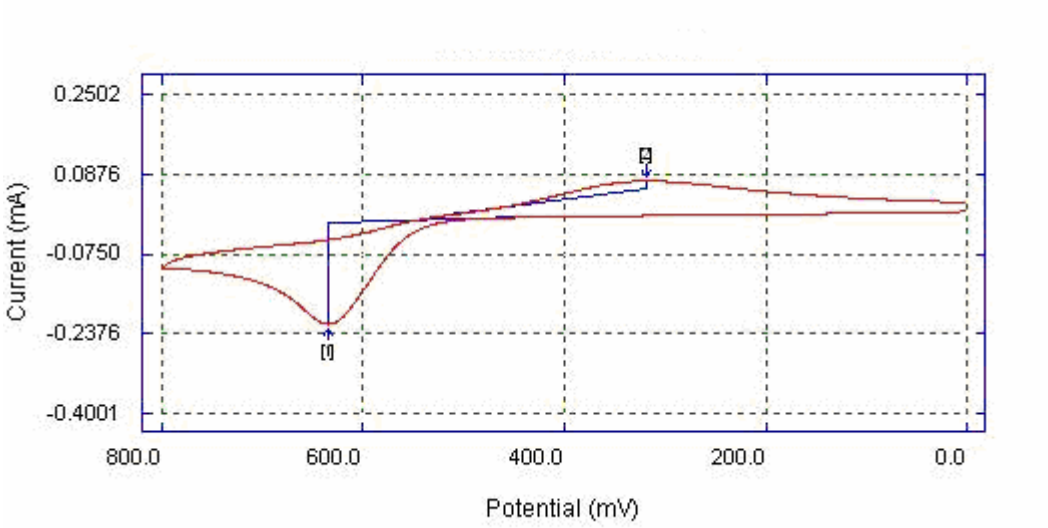

Figure 16. Cyclic voltammogram of 5mM CAT in 0.01 M sulfuric acid at a P3MT GCE grown at 1500 mV. Scan rate = 100 mV/s.

Also as evidenced by the values in Table 3, the SGC/TiO_2 electrode permits a shorter response time in the electrochemical oxidation of AA as compared to the P3MT modified GCE and the bare GCE. There is a significant decrease of oxidation overpotential at the SGC/TiO_2 electrode. Cyclic voltammograms for AA oxidation at the SGC/TiO_2 electrode and 1800 mV P3MT modified GCE are shown in Figures 17 and 18. The decrease in oxidation potential at the P3MT modified electrode has been tested in

similar studies using other conductive polymers. [38] The faster response time exhibited at the SGC/TiO_2 electrode can be attributed to the higher mass transport rate at the smaller size electrode. The higher mass transport rate at the smaller size SGC reduces the detection limit of the analytes CAT and AA and permits a short response time. P3MT coating inhomogeneity on the electrodes tip varies the locations of active sites available for electron transfer. Also, varying voltage during electropolymerization varies the number of active sites within the multi-layered polymer coating. This also contributes to the poorer response time.

Table 3

Cyclic voltammetric peak potentials for catechol[a] and ascorbic acid[a] in sulfuric acid[a]

	Catechol			Ascorbic Acid
Electrode	E_p(a) (mV)	i_a/i_c [e]	ΔE (mV)[b]	E_p(a) (mV)
SCG/TiO_2	513	1.05	84	280
	185[d]	2.70	59[d]	
P3MT				
1.8 V[c]	598	1.95	191	483
1.65 V[c]	639	4.37	250	513
1.5 V[c]	657	13.70	274	563
Bare	--		--	--

[a]Catechol, ascorbic acid, and sulfuric acid concentrations were 5, 5 and 100 mM respectively. Scan rate = 100 mV/s.
[b] ΔE = Peak potential difference between anodic and cathodic peaks.
[c] Values shown represent the voltage applied during electropolymerization.
[d] Values for Catechol in phosphate buffer solution, pH 6.82
[e] Peak current ratios determined from anodic peak and cathodic peak values

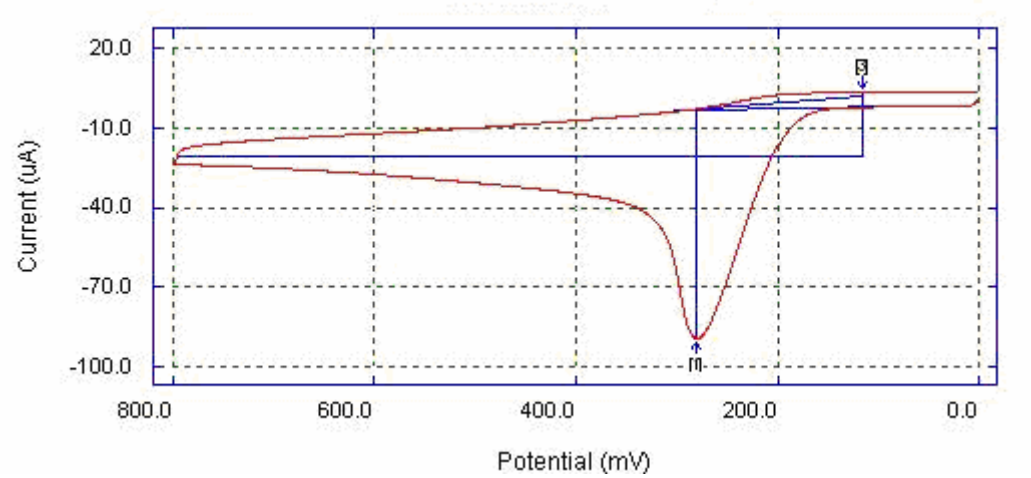

Figure 17. Cyclic voltammogram of 5mM AA in 0.01 M sulfuric acid at a SGC/TiO_2 electrode. Scan rate = 100 mV/s.

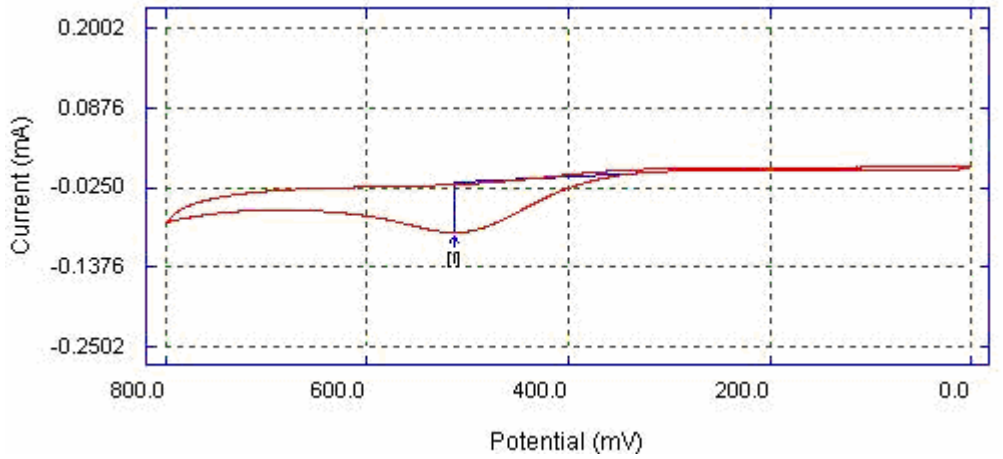

Figure 18. Cyclic voltammogram of 5mM AA in 0.01 M sulfuric acid at a P3MT GCE. Scan rate = 100 mV/s.

Response specificity

Specificity of response is a desirable property in sensors. The ability to fine tune the microstructure of the chemical immobilized on the electrode tip could possibly be used as a size-exclusion method to discriminate against interfering molecules. [10] In terms of sol-gel methods, amphiphilic organic molecules such as surfactants and block copolymers have been used in target specific applications to fabricate highly porous

materials with a desired pore structure and size. [28] In the case of conductive polymers they are often plagued with uneven distribution of the polymer layers on the surface of the electrode. The cyclic voltammograms in Figures 19, 20**,** and 21 illustrate the selectivity principle in the electrochemical detection of catechol in the presence of ascorbic acid.

As mentioned prior, the detection of catechol can be effected by the presence of ascorbic acid. It is the electrodes selectivity that accounts for its ability to detect catechol in the prescence of ascorbic acid. Figure 21 shows clearly that the SGC/TiO_2 electrode was able to electrocatalyze the oxidation of catechol in the presence of ascorbic acid. The oxidation peaks of catechol and ascorbic acid are being resolved and the reduction peak is detected. However, the cyclic voltammograms at the bare carbon electrode as designated in Figure 19, illustrates that the oxidation peaks of catechol and ascorbic acid are not resolved, and the reduction and oxidation peaks for catechol are not detectable. Looking at Figure 19 against Figures 20 and 21, both the P3MT modified electrode and the SGC/TiO_2 electrode, improve the electrochemical detection of catechol in the presence of ascorbic acid. At the P3MT modified electrode however, CV shown in Figure 20, there appears to be an oxidation and reduction peak measured for catechol, without clear resolution for the oxidation peak of AA. The peak separation is not as evident for the catechol/ascorbic acid mix at the P3MT modified electrode as observed at the SGC/TiO_2 electrode. Previous research conducted using the sol-gel method for the synthesis of thin films, has described the ability of the sol-gel matrix to act as a possible size exclusion method. [39] The pore size of conductive polymers can not be fine tuned in the same way as the sol-gel matrix. As a result of this, the P3MT modified electrode was

unable to discriminate against the larger interfering ascorbic acid molecules resulting in the CV shown in Figure 20.

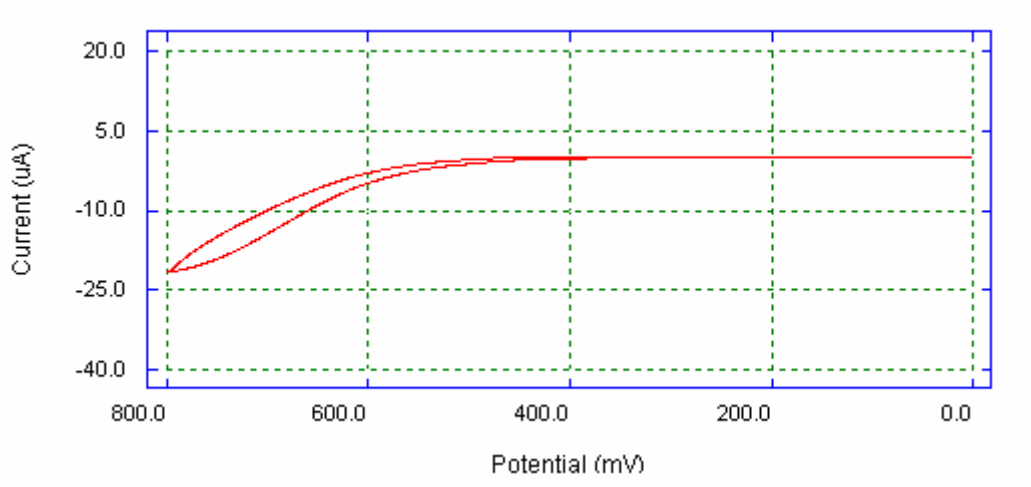

Figure 19. Cyclic voltammogram of 5mM CAT + 5mM AA in 0.01 M sulfuric acid at a bare GCE. Scan rate = 100 mV/s.

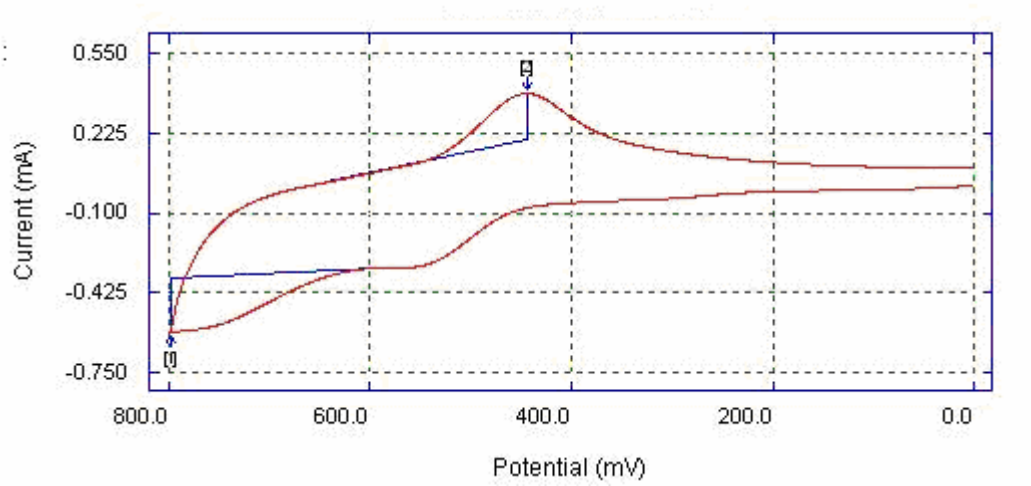

Figure 20. Cyclic voltammogram of 5mM CAT + 5mM AA in 0.01 M sulfuric acid at a P3MT GCE. Scan rate = 100 mV/s.

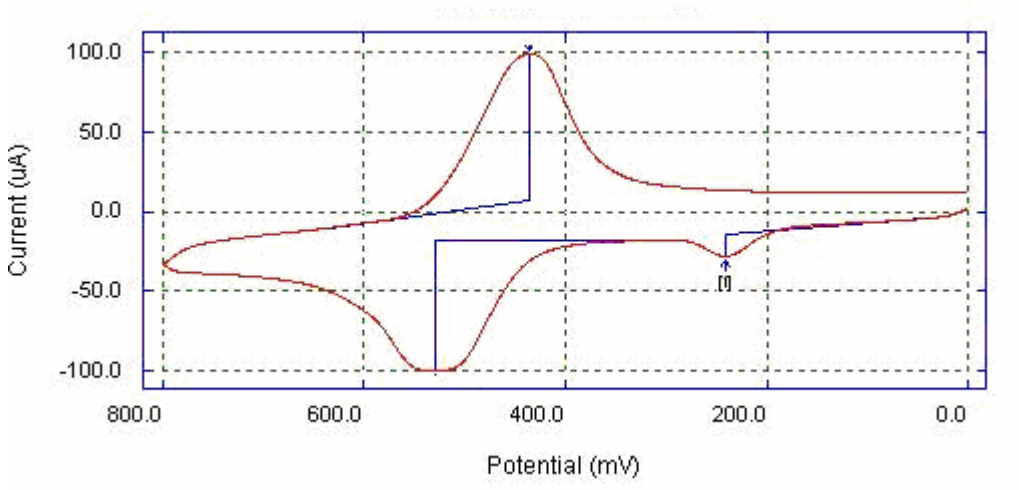

Figure 21. Cyclic voltammogram of 5mM CAT + 5mM AA in 0.01 M sulfuric acid at a SGC/TiO_2 electrode. Scan rate = 100 mV/s.

Sensor Stability

A basic requirement of sensor behavior is that a fixed output be maintained over time when the sensor is exposed to a constant concentration of analyte. In the context of sol-gel sensors and conductive polymer sensors, two factors affect the sensor stability. First a fully stabilized microstructure of the host matrix must be achieved for both sol-gel and conductive polymer sensors before the sensor is used. Alterations in the microstructure will likely manifest changes in sensor response. The second and of greatest importance is the leaching of the electroactive species from the electrode surface. This can be problematic during liquid-phase sensing. Contraction of the microstructure helps to diminish the probability of leaching occurrence, however the decrease pore size that accompanies contraction, reduces permeability and as a result the response time.

The repeatability of the response relative to catechol oxidation process on the P3MT modified electrode and the SGC/TiO_2 electrode was tested by repeatedly scanning the potential from 0 to 800 mV, in 0.01M sulfuric acid solution containing 5mM CAT.

The stability was tested by series of 20 consecutive scans. Repetitive voltammograms from a 5mM catechol solution were registered at both the P3MT modified GCE and a SGC/TiO_2 electrode. The voltammograms recorded on the first scan is different from the subsequent ones for both the P3MT modified electrode and the SGC/TiO_2 electrode. With on going cycling, the current changes at both electrodes. As Figure 22A and Figure 22B illustrate, after 20 consecutive scans, the changes were prominent at the P3MT modified electrode. In comparing the changes in current after 10 scans, the peak current changed slower at the SGC/TiO_2 electrode. At the P3MT modified electrode, the current changed from 0.1839 mA, at scan 2 to 0.2330 mA at scan 10. This represents a 21% loss of the initial signal at the P3MT modified electrode. At the SGC/TiO_2 electrode, the current changed from 0.0823 mA at scan 2 to 0.0866 mA at scan 10, representing a 5% loss of the initial signal at the SGC/TiO_2 electrode. The current/ signal variation exhibited suggests a progressive degradation of the coating from the electrode tip. A proposed conclusion is that the P3MT adherence to the sonogel carbon electrode surface weakens as the number cycles increase; exhibiting instability. It also indicates a higher resistance to the electrode fouling for the SGC/TiO_2 electrode.

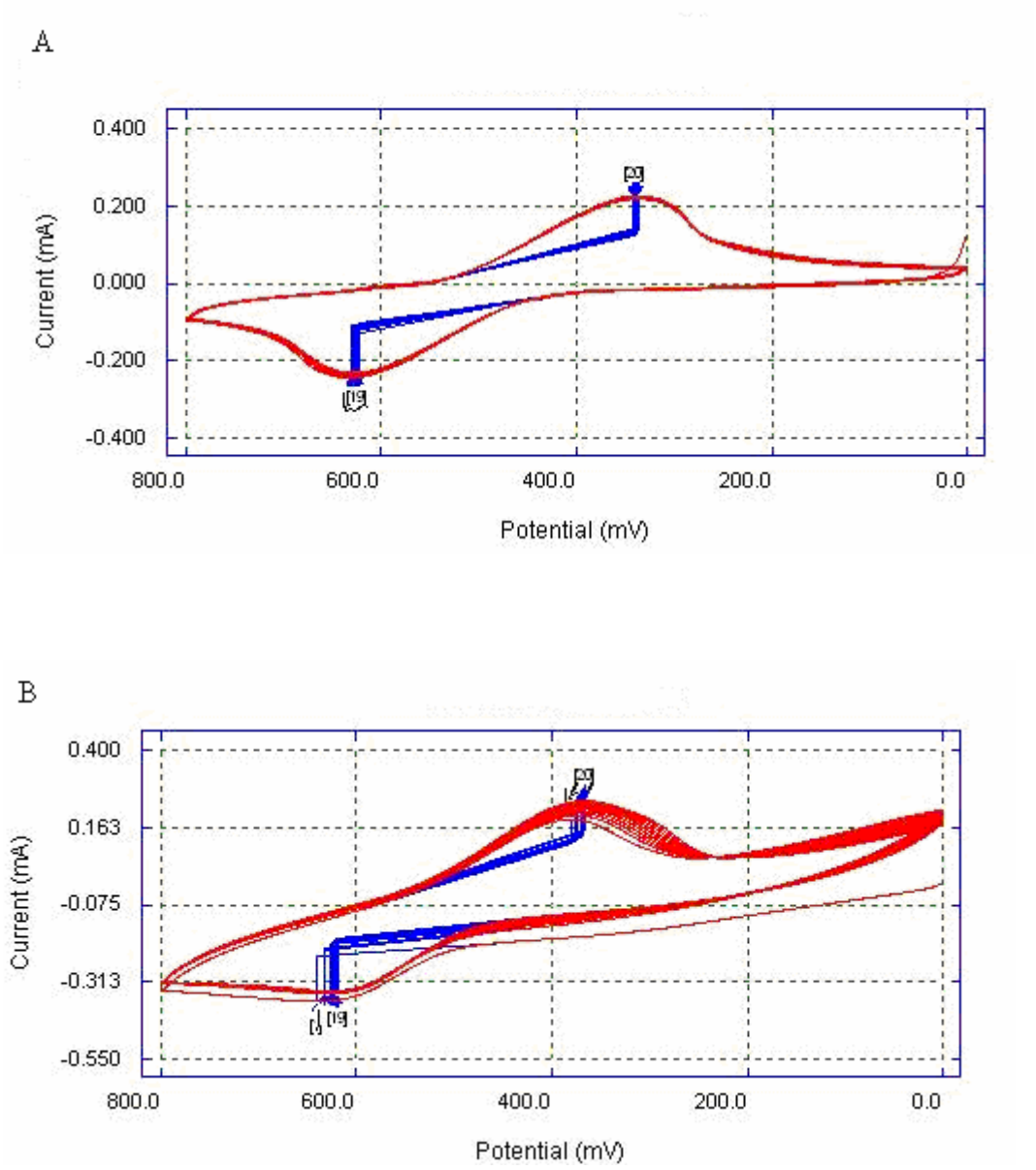

Figure 22. Cyclic voltammogram stability comparison of (A) SGC/TiO_2 and (B) P3MT modified electrode in the detection of 5mM catechol in .01 M sulfuric acid over 20 scans. Scan Rate = 100 mV/s.

Susceptibility to interferents

For straight forward one-electron outer sphere electron-transfer reactions at electrodes, the choice of metallic electrode material has only a minor effect upon the rate of the electron-transfer reaction. [25] For reactions involving multiple electron transfers

and associated formation or breaking of chemical bonds, the choice of electrode material can have a profound effect on the rate of the electrode reaction. Electron transfers precede in sequence one electron at a time. The stabilization of the one-electron intermediate plays a significant role in determining the overall reaction rate. This problem arises in the electrochemical oxidation of NADH. NADH oxidation follows the ECE mechanism. This mechanism involves electrochemical (E) generation of a species, in this case a cation radical $NADH^{+\bullet}$, that interacts with solution components (C). The $NADH^{+\bullet}$ radical is more easily oxidized than the starting material and is immediately electrolyzed (E). In aqueous solution NADH is converted to NAD^+.

The overall reaction steps are [16]:

$$NADH \rightarrow NADH^{+\bullet} + e^-$$
$$NADH^{+\bullet} \rightarrow NAD^{\bullet} + H^+$$
$$NAD \rightarrow NAD^+ + e^-$$

If not stabilized this intermediate can interfere with NADH oxidation and can inhibit the oxidation process. As a result of this, there may be more than one anodic peak present in voltammograms, as well as oxidation may occur at high overpotentials. To address this problem, chemically modified electrodes have been used, in which the reactant in solution undergoes oxidation or reduction by chemical reaction with the immobilized mediator at the surface of the electrode. The key to the success of this strategy is finding a way to immobilize the mediator on the electrode surface without limiting the catalytic process. In this study PBTP and P3MT modified GCEs were used for this purpose as well as the sol-gel method. The use of sol-gels for this purpose has obtained high interest because they can obtain ceramic inorganic materials in a process at low temperature, providing perfect matrices to incorporate highly sensitive and selective

molecules. [27] The response time of sol-gel and conductive polymer coated sensors is generally associated with the time required for an analyte to diffuse through the immobilized chemical matrix found at the electrode tip. This problem can be amplified by electrostatic interactions between the matrix and charged analytes.

As shown in Figure 23 and Figure 24, at both the bare GCE and PBTP modified GCE two anodic peaks are present in cyclic voltammogram of the oxidation of NADH.

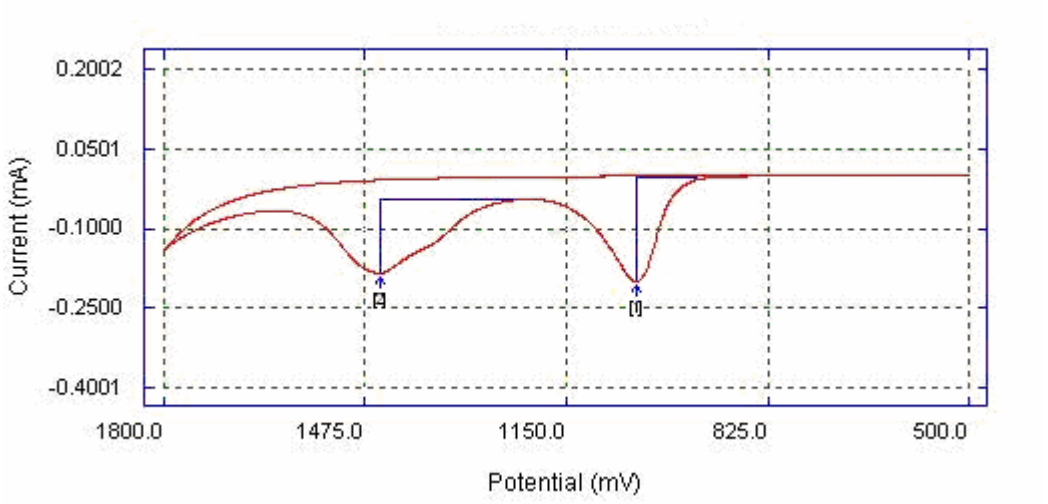

Figure 23. Cyclic voltammogram of 5mM NADH in 0.1 M Phosphate Buffer pH 6.82 at a PBTP GCE. Scan rate = 50mV/s.

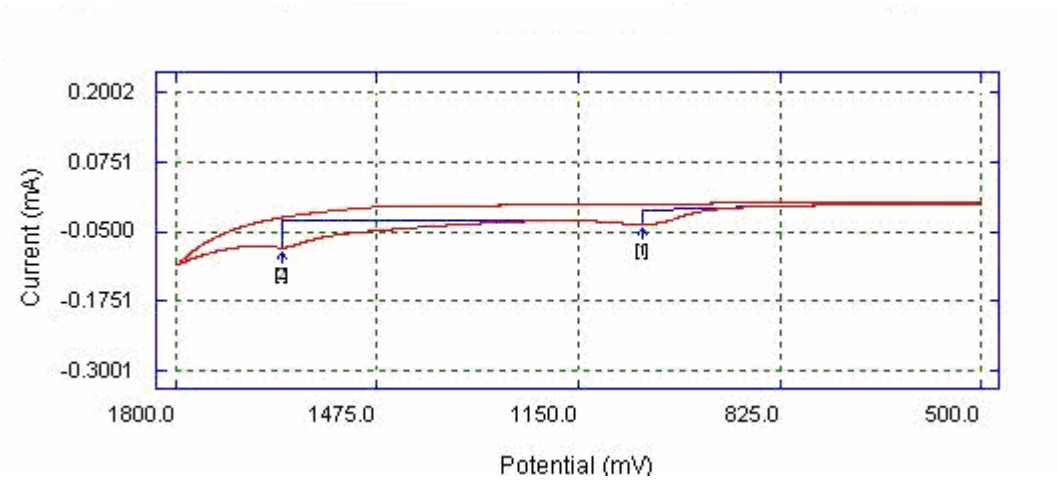

Figure 24. Cyclic voltammogram of 5mM NADH in 0.1 M Phosphate Buffer pH 6.82 at a bare GCE. Scan rate = 50 mV/s.

At the SGC/TiO_2 electrode, shown in Figure 25, there is only one anodic peak.

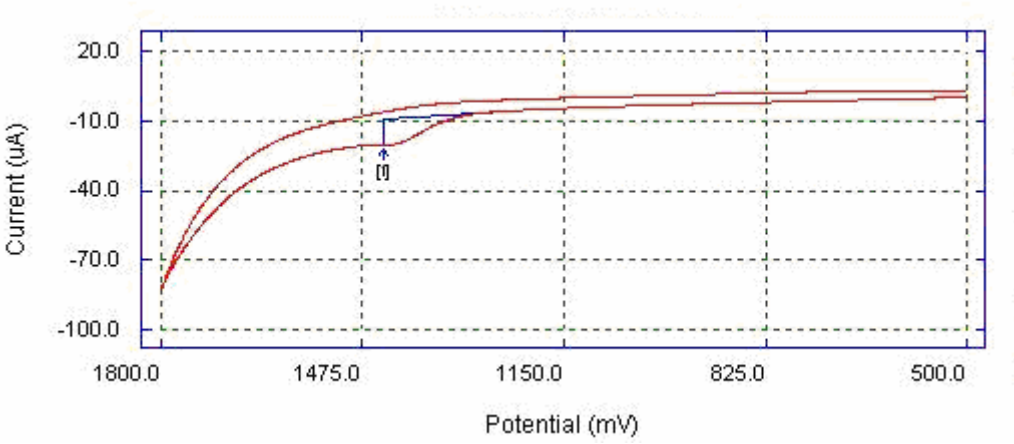

Figure 25. Cyclic voltammogram of 5mM NADH in 0.1 M Phosphate Buffer pH 6.82 at a SGC/TiO_2 electrode. Scan rate = 50 mV/s.

Electrode performance is measured by the ability of the electrode to stabilize the intermediate steps. The presence of two anodic peaks at the PBTP modified electrode and bare GCE agree with similar mechanistic conclusions using platinum modified electrodes. [39] Peak 1 is due to the formation of the unstable intermediate $NADH^{+\cdot}$, peak 2 is the NAD^+ peak. At the PBTP modified electrode and bare electrode, there are two anodic peaks present, demonstrating the inability of the PBTP modified GCE and bare GCE to stabilize the interference due to NAD^+. The SGC/TiO_2 electrode was able to detour the susceptibility to interfering NAD^+, therefore one anodic peak was present in the voltammogram. The direct electrochemical oxidation of NADH at the bare electrode and PBTP modified electrode proceeded at higher overpotentials than at the SGC/TiO_2 electrode. At the SGC/TiO_2 electrode electrochemical oxidation occurred at 1452 mV. At the bare GCE, electrochemical oxidation occurred at 1593 mV. At the PBTP modified electrode, electrochemical oxidation occurred at 1463 mV. In comparing the electrochemical response of the SGC/TiO_2 electrode with the bare GCE, there was a

potential decrease of 141 mV using the SGC/TiO_2 electrode. In comparing the bare GCE to the PBTP modified GCE there was a potential decrease of 130 mV. The TiO_2 is a better mediating species than 2,2(bithiophene) in the electrochemical oxidation of NADH.

Electrolyte and Scan Rate Effects on NADH detection

The background electrolyte itself had a marked effect upon the anodic peak separation and positions for NADH at both the SGC/TiO_2 electrode and the PBTP modified electrode. The solvent used can be one that the newly deposited polymeric film interacts with favorably. When it favorably interacts, the film swells and become porous facilitating more transfer of electrons. On the other hand, the film can interact unfavorably in which case it can form a resistive layer that impedes penetration of electrons. Anodic peak potential values in Table 4 for NAD+ demonstrate that acids improve the irreversible behavior of NADH when compared to their sodium salts at PBTP modified electrodes. It is within the more acidic electrolyte solutions that the detection of NADH occurs at lower potentials. The improvement is of dramatic size at the PBTP electrode. In sulfuric acid the NADH anodic peak is found at 1080 mV. In sodium sulfate, the NADH anodic peak has a potential of 1627 mV. NADH anodic peak position shifted to a less positive position by 547 mV, in the acid. The SGC/TiO_2 electrode exhibited behavior opposite of the PBTP modified electrode. In sulfuric acid the NADH anodic peak position is at 1496 mV. In sodium sulfate, the NADH anodic peak position is at 1440 mV. It appears that the Titanium (IV) Oxide matrix interacted more favorably with sodium sulfate. As a result of favorable interactions, anodic peak potential value in sodium sulfate was 56 mV less than in sulfuric acid. The shift in peak

position is not as dramatic at the SGC/TiO_2 electrode as is seen at the PBTP modified electrode. In terms of highest anodic peak potentials, at the PBTP modified electrode, the highest peak potential of 1782 mV was measured in sodium nitrate. The highest anodic peak potential of 1496 mV at the SGC/TiO_2 electrode was recorded in sulfuric acid. The relatively higher oxidation potential for NADH at the PBTP modified electrode observed in sodium nitrate agrees with earlier works involving the use of conducting polymer coated electrodes. [37]

When considering the potential gradient that exist across the electrochemical cell, we find that it exists only in the narrow interphase regions near the surfaces of the working and auxillary electrodes. Comparing electrolytes with varying ionic strengths, one would expect the electrolyte solution with highest strength, to be able to carry more ions towards the electrodes. The potential would decay more quickly than in an electrolyte with weak ionic strength. This is expected from the Debye-Huckel theory. In electrolytes with higher ionic strength, there is a time averaged distribution of ions closer to the surface of the electrode, whereas at low ionic strength, the thermal agitation competes more effectively and the time-averaged distribution of an ion excess extend further from the surface. So there are less charge carriers and the response time would be poorer. The Epsilon (Bioanalytical Systems) electrochemical workstation employed in this investigation was unable to detect NADH in sodium nitrate at a SGC/TiO_2 electrode.

Table 4

Electrolyte effect on the cyclic voltammetric peak potentials and currents for NADH

Electrolyte[a]	SGC/TiO_2		PBTP	
	E_p(a) (mV)	i (mA)	E_p(a) (mV)	i (mA)[b]
Sulfuric acid	1496	.2332	1080	.0181
Sodium sulfate	1440	.1134	1046,1627[b]	.0490
Nitric acid	1187	.0470	1280	.0114
Sodium nitrate	-	-	1322,1782[b]	.2958
Phosphate Buffer pH 6.82	1452	.01046	1030, 1463[b]	.0739

[a] NADH and electrolyte concentrations were 5 and 100 mM, respectively. Scan Rate = 50mV/ s.
[b] NADH oxidation peak values. Additional peak due to NAD+ interferent.

Cyclic voltammograms of 5mM NADH at a PBTP modified GCE yielded non-linear peak current (i_p) versus scan rate (ν) $^{1/2}$ plots for potential scan rates between 25 and 100 mV s^{-1} (Figure 26), indicating lack of diffusion control of the oxidation current under these conditions. These results agree with those previously reported. [41] Moreover the plot of log i_p versus log ν (Figure 26) showed a linear dependence (r = 0.9804) between 25 and 100 mV s^{-1}. This suggests a mixed diffusive-adsorptive control of the NADH oxidation current. For potential scan rates higher than 50 mV s^{-1} , cyclic

voltammograms were distorted, indicating the possible involvement of adsorption processes onto the electrode surface. At scan rates below 50 mV s^{-1} the SGC/TiO_2 electrode was unable to detect NADH. No cathodic peaks appeared in the potential range scanned in any case, and peak potential was shifted towards more positive values when the scan rate increased which indicated non-reversibility of the NADH oxidation.

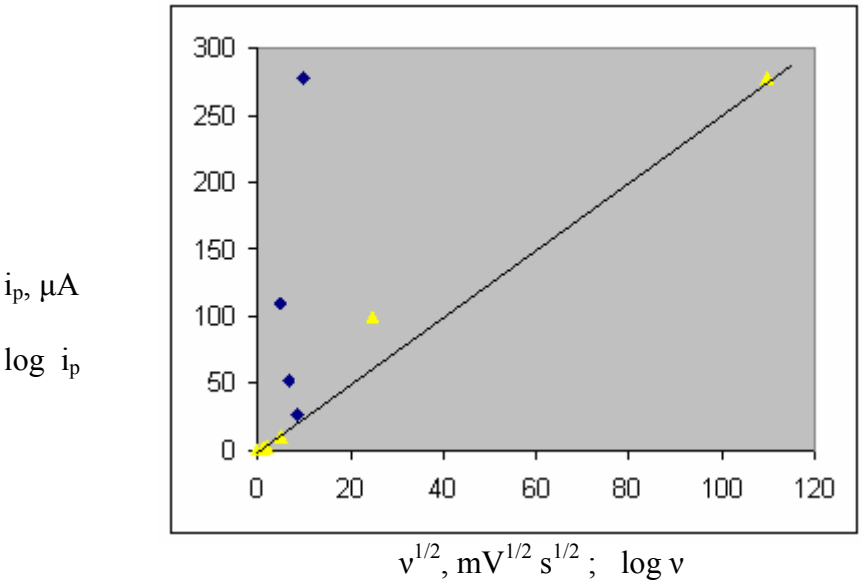

Figure 26. Influence of the potential scan rate on the NADH peak current obtained by cyclic voltammetry at a PBTP coated GCE: (diamonds) i_p versus $\nu^{1/2}$ plot; (triangles) log i_p versus log ν plot; 5mM NADH in 0.1 M phosphate buffer, pH 6.82.

APPENDIX

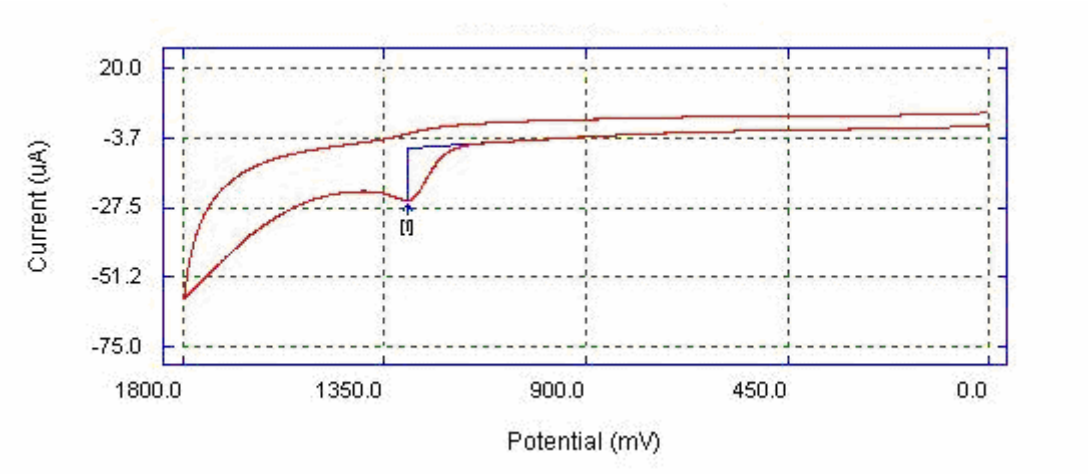

Cyclic voltammogram of undoping of PBTPGCE in 0.1 M TBATFB/ACN.
Scan Rate = 100 mV/s

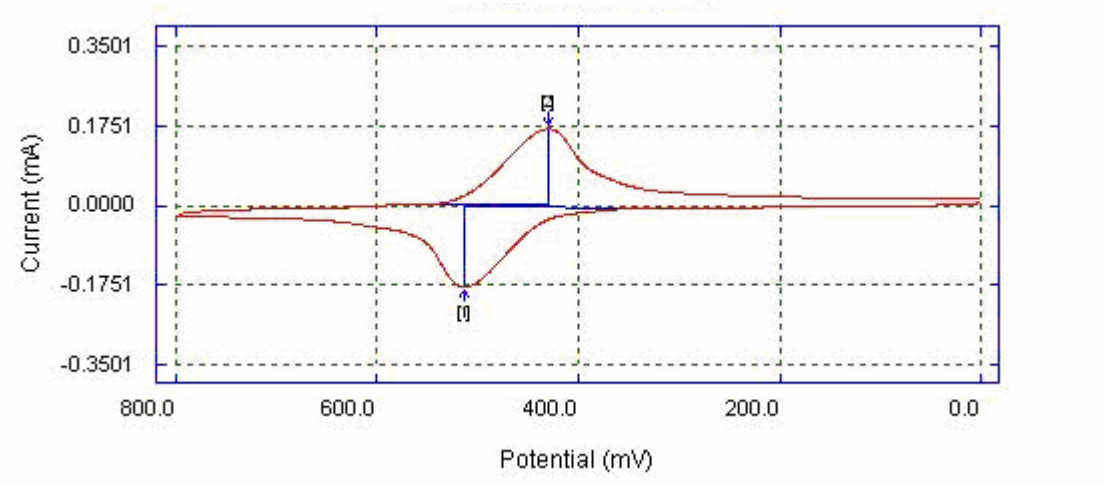

Cyclic voltammogram of 5mM catechol in 0.01M sulfuric acid at a sonogel carbon electrode modified with Titanium (IV) Oxide (SGC/TiO_2). Scan rate = 100 mV/s.

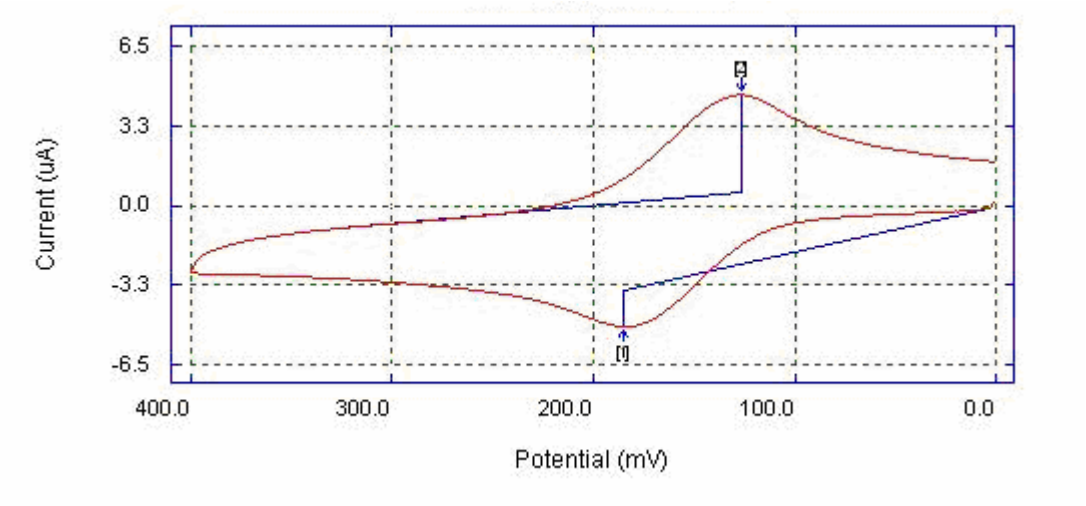

Cyclic voltammogram of 5mM CAT in 0.1M Phosphate Buffer, pH 6.82 at a SGC/TiO_2 electrode. Scan Rate = 100 mV/s.

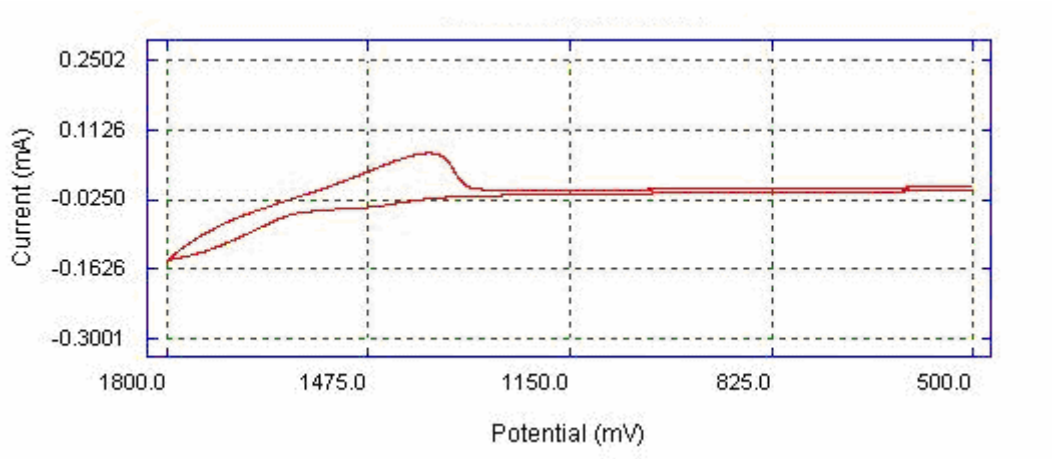

Cyclic voltammogram of 5mM NADH in 0.1 M sodium nitrate at a SGC/TiO_2 electrode. Scan rate = 50 mV/s

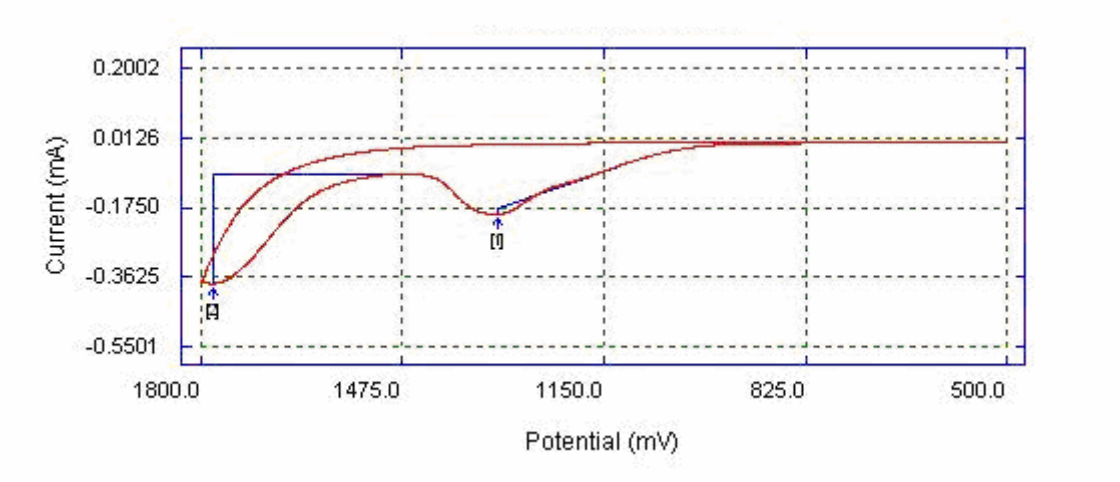

Cyclic voltammogram of 5mM NADH in 0.1 M sodium nitrate at a PBTP modified electrode. Scan rate = 50 mV/s

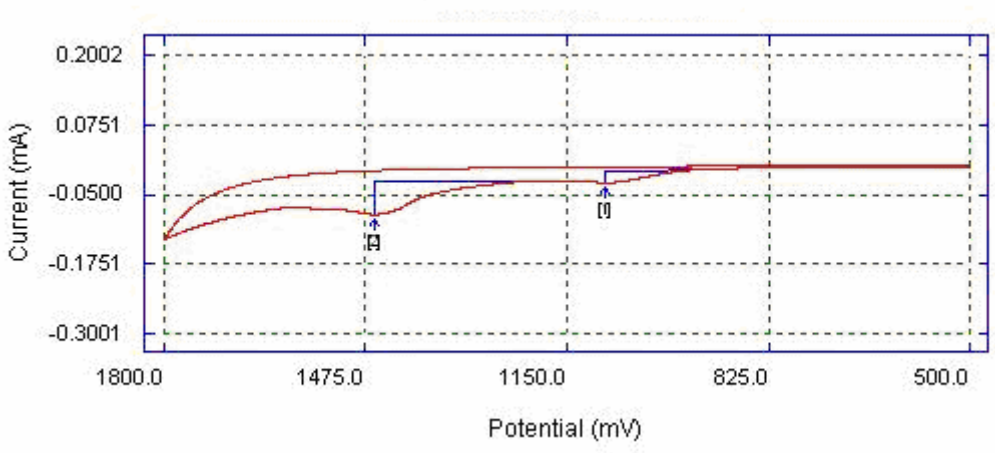

Cyclic voltammogram of 5mM NADH in 0.1 M sodium sulfate at a PBTP modified electrode. Scan rate = 50 mV/s.

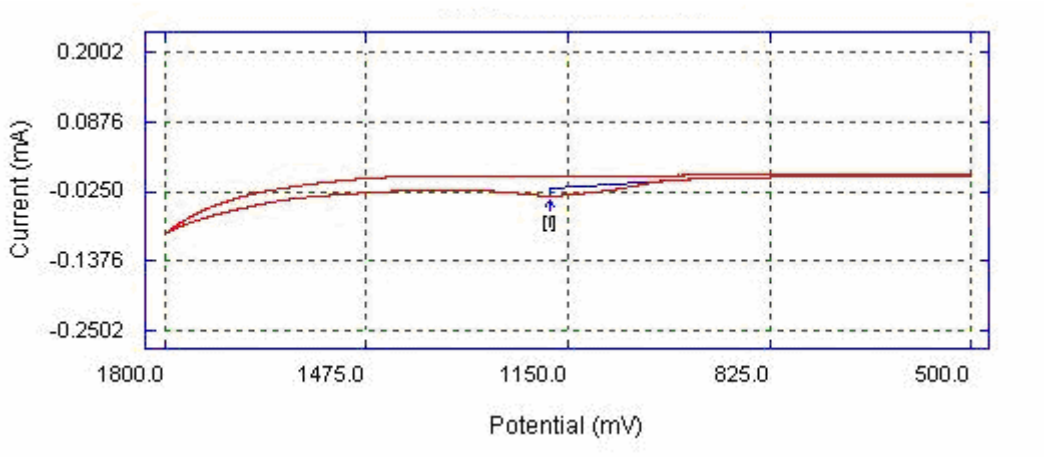

Cyclic voltammogram of 5mM NADH in 0.1 M nitric acid at a SGC/TiO_2 electrode. Scan rate = 50mV/ s.

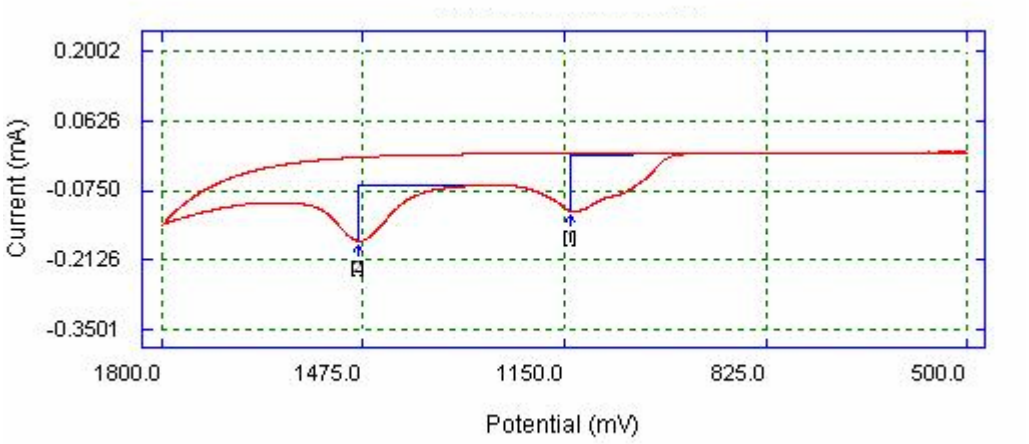

Cyclic voltammogram of 5mM NADH in 0.1 M phosphate buffer pH 6.82 at a PBTP modified electrode. Scan rate = 25 mV/s.

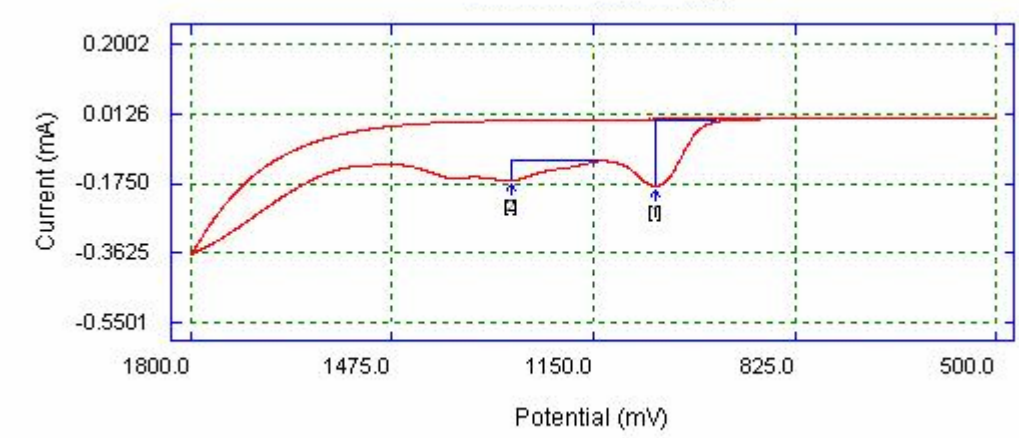

Cyclic voltammogram of 5mM NADH in 0.1 M phosphate buffer pH 6.82 at a PBTP modified electrode. Scan rate = 50 mV/s.

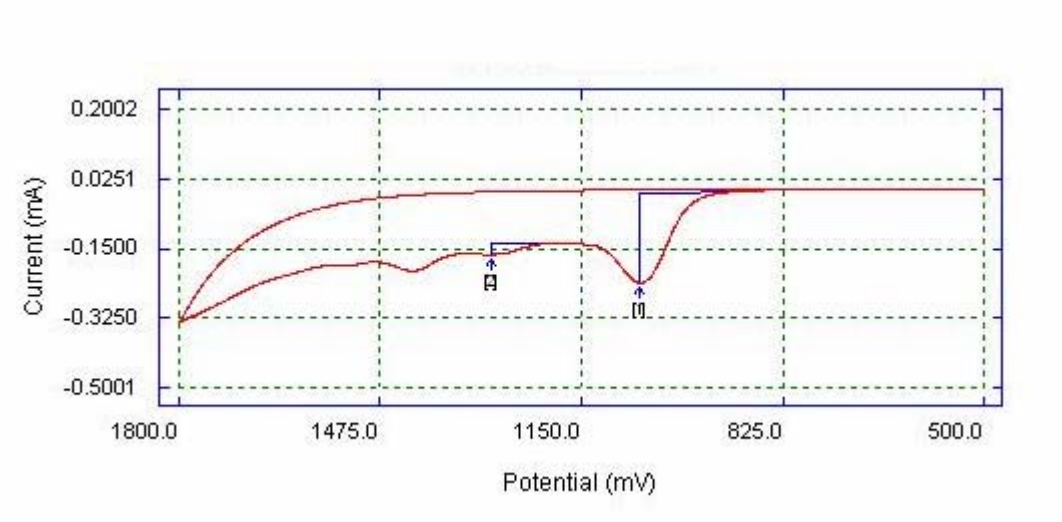

Cyclic voltammogram of 5mM NADH in 0.1 M phosphate buffer pH 6.82 at a PBTP modified electrode. Scan rate = 75 mV/s.

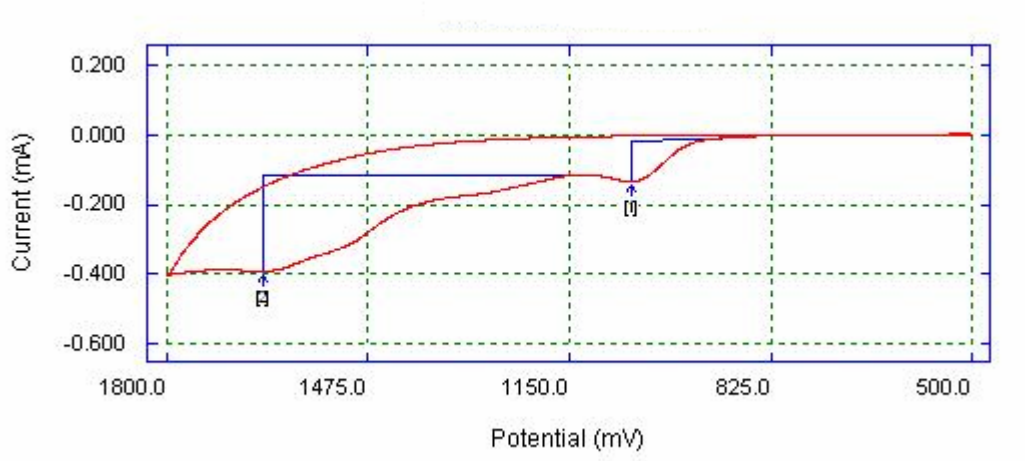

Cyclic voltammogram of 5mM NADH in 0.1 M phosphate buffer pH 6.82 at a PBTP modified electrode. Scan rate = 100 mV/s.

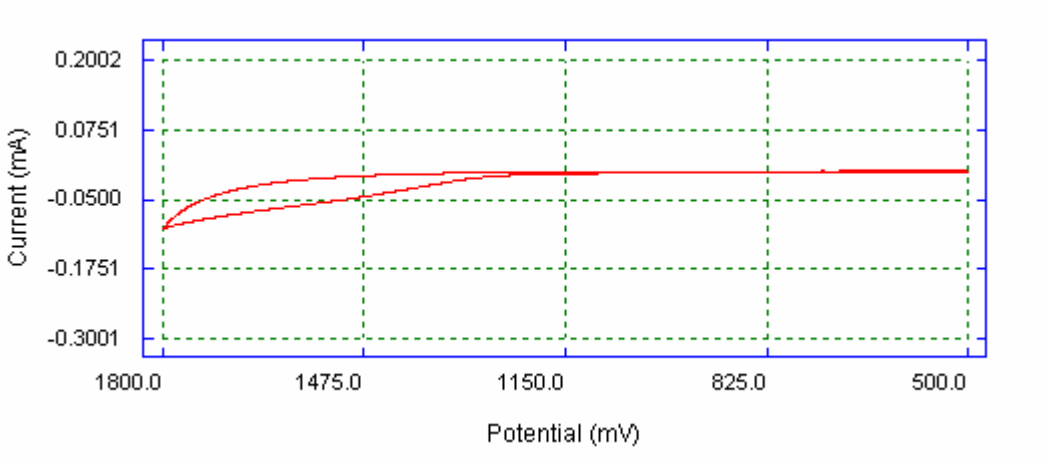

Cyclic voltammogram of 5mM NADH in 0.1 M phosphate buffer pH 6.82 at a SGC/ TiO_2 electrode. Scan rate = 25 mV/s.

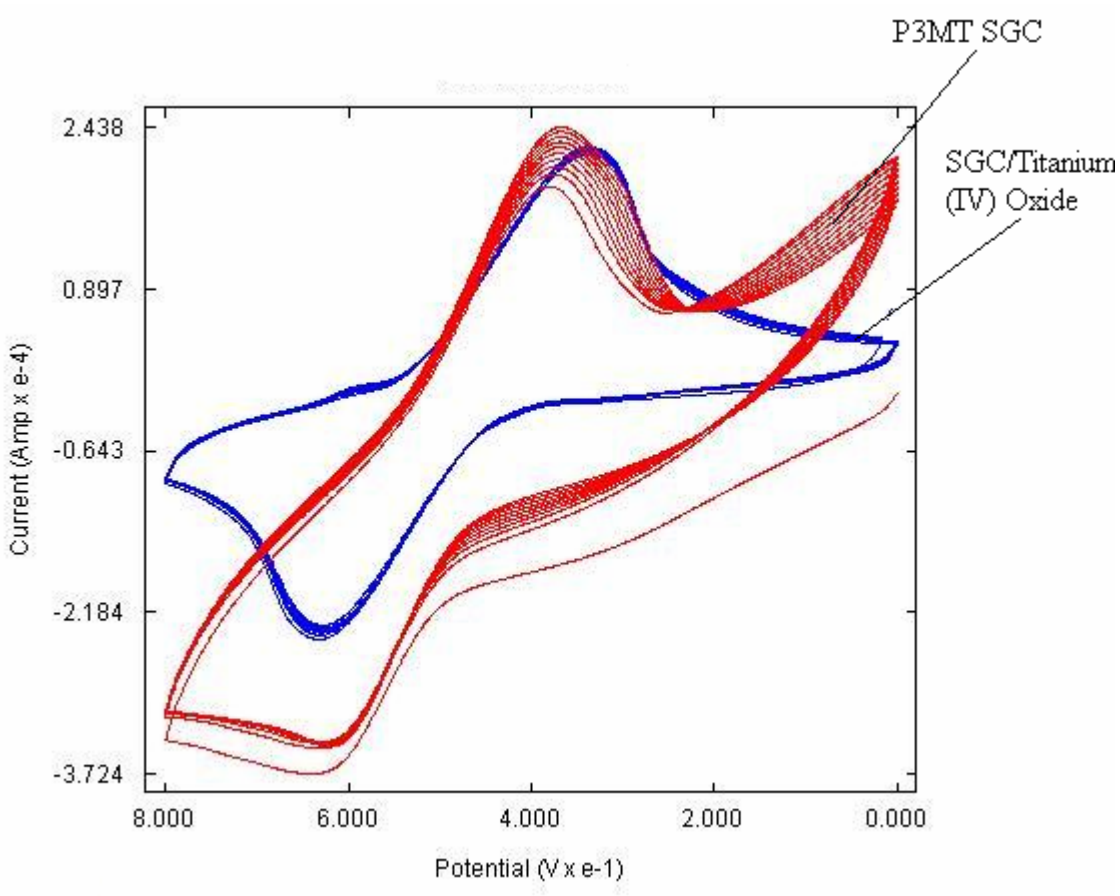

SGC/TiO_2 electrode and P3MT modified SGC stability cyclic voltammogram overlay. 5mM CAT in 0.1 M sulfuric acid. 20 consecutive scans. Scan rate = 100mV/s.

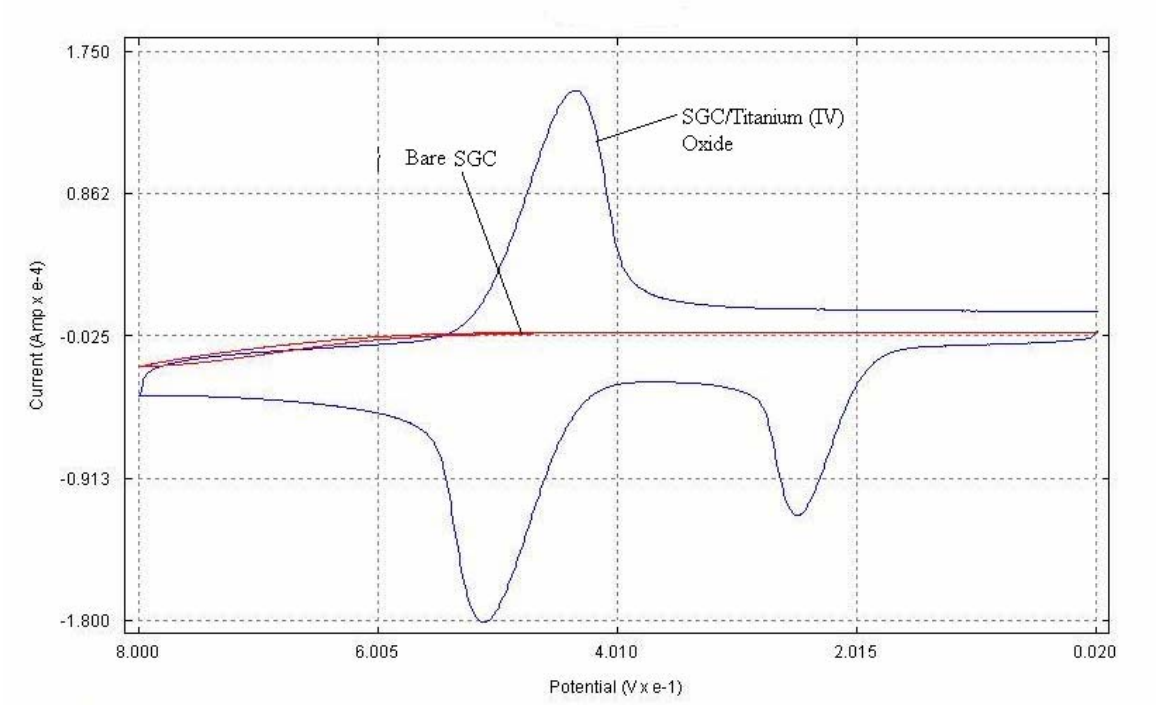

Bare SGC and SGC/TiO_2 electrode cyclic voltammogram overlay.
5mM catechol + 5mM Ascorbic Acid in 0.01M sulfuric acid. Scan rate = 100 mV/s.

List of References

REFERENCES

1.Heineman, W. R., Kissinger, P.T., *Laboratory Techniques in Electroanalytical Chemistry*, Second Edition, Marcel Dekker: Inc., New York, 1996; pp. 29,47-49.

2. Fry, A.J., Britton, W.E., Topics in Organic Electrochemistry, Plenum Press: New York, 1986; p.255.

3. Moses, P.R., Wier L., and Murray R.W., *Anal. Chem.* **47**, 1882 (1975).

4. Watkins, B.F., Behling J.R., Kariv, E., and Miller, L.L., *J. Am. Chem. Soc.* **97**,3549 (1975).

5. Miller, L.L.; Van De Mark, M. R., *J. Am. Chem. Soc.* **100**, 639-640, (1978).

6. Naegeli, R.; Redepenning, J.: Anson, F.C. *J Physical Chemistry* **90**, 6227-6232, (1986).

7. Kaufman, F. B.; Engler, E.M. *J. Amer. Chem. Soc.*, **101**, 547-549, (1979).

8. Guadalupe, A. R.;Abruna, H.D. *Anal. Chem.* **57**, 142-149, (1985).

9. Fleishmann, M.; Pons, S.; Rolison, D. R.; Schmidt, P.P., Eds. *Ultramicroelectrodes*;. Datatech Systems: Morgantown, NC, 1987.

10. Brinker, C.J.; Scherer, G.W., *Sol-Gel Science, The Physics and Chemistry of Sol-Gel Processing* ; Academic Press: New York, 1990.

11. Salamone, Joseph C., *Concise Polymeric Materials Encyclopedia;* CRC Press: Boca Raton, FL, 1999; pp. 259-261, 1575.

12. Wang, Joseph, *Analytica Chimica ACTA*, **399**, 21-27, (1999).

13. H.B. Mark, Jr., N.F. Atta, Y.L. Ma, K.L. Petticrew, H. Zimmer, Y. Shi, S.K. Lunsford, J.F. Rubinson, A. Galal *Bioelectrochem. Bioenerg.,* **38**: 229, (1995).

14. P. Jaraba, L. Agui, Yanez-Sedeno, J.M. Pingarron, *Electrochemica*, **43,** 3555- 3565 (1998).

15. N. Alvarez, P. Ortea, A. Paneda, M.J. Lobo Castanon, A.J. Miranda Ordieres, P. Tunon Blanco, *Journal of Electroanalytical Chemistry*, **502**, 109-117 (2001).

16. R.L. Blankespoor, L. Miller, *Journal of Electroanalytical Chemistry and Interfacial Electrochemistry*, **171**, 231-241 (1984).

17. B. Carlson, L.L. Miller, P. Neta, J. Grodkowski, *J. Am. Chem. Soc*., **106**, 7233-7239 (1984).

18. J. Wang, P. Pamidi, M. Jiang, *Analytica Chimica Acta*, **360**, 171-178, (1998).

19. C. Retna Raj, S. Behera, *Biosensors and Bioelectronics*, **21**, 949-956, (2005).

20. J. Chen, J. Bao, C. Cai, T. Lu, *Analytica Chimica*, **516**, 29-34, (2004).

21. M. del Mar Cordero-Ro, J.L.H-H. Cisneros, E. Blanco, I.I. Naranjo-Rodriguez, *Anal. Chem.*, **74**, 2423, (2002).

22. Lunsford, S.K., Choi H., Stinson J., Yeary A., Dionysiou, D.D., *Talanta*; Elsevier B.V.: (2007).

23. C.Wang, Z.X. Deng, Y. Li, *Inorg. Chem*, **40**, 5210, (2001).

24. H. Choi, A.C. Sofranko, D.D. Dionysiou, *Adv. Funct. Mater.*, **16**, 1067, (2006).

25. J. Wang, P.V.A. Pamidi, M. Jiang, *Analytica Chimica Acta*, **360**, 171-178, (1998).

26. S. Gosavi, R.A. Marcus, *J. Phys. Chem. B*, **104**, 2067-2072, (2000).

27. J.A. Rodriguez, M.D. Petit Dominguez, J.M. Pinilla Macias, *Analytica Chimica Acta*,**524**, 339-346, (2004).

28. H. Choi, E. Stathatos, D.D. Dionysiou, *Thin Solid Films*, Elsevier B.V., (2005).

29. F. Bosc, D. Edward, N. Keller, V. Keller, A. Ayral, *Thin Solid Films***, 495**, 272, (2006).

30. H. Choi, E. Stathatos, D.D. Dionysiou, *Thin Solid Films*, **510**, 107, (2006).

31. S.T. Martin, J.M. Kesselman, D.S. Park, N.S. Lewis, M.R. Hoffman, *Environ. Sci. Technol.*, **30**, 2535, (1996).

32. S. Mu, *Biosens. Bioelectron.*, **21**, 1237, (2006).

33. S. Dong, T. Kuwana, *J. Electrochem. Soc.*, **6**, 617, (1994).

34. J. Wang, P. Pamidi, M. Jiang, *Anal. Chem. Acta*, **360**, 171, (1998).

35. Razmi, M. Agazadeh, B. Habibi, *J. Electroanal. Chem.*, **547**, 25, (2003).

36. H. Qi, C. Zhang, *Electroanalysis*, **17**, 832, (2005).

37. R.A. Saraceno, J.G. Pack, A.G. Ewing, *J. Electroanal Chem.*, **197**, 265-278, (1986).

38. S. Lupu, A. Mucci, L. Pigani, R. Seeber, C. Zanardi, *Electroanalysis*, **14**, 519-524, (2002).

39. B.D. MacCraith, C. McDonagh, A.K. Mcevoy, T. Butler, G. O'Keeffe, V. Murphy, *Journal of Sol-Gel Science and Technology*, **8**, 1053-1061, (1997).

40. W.J. Blandel, R.A. Jenkins, *Anal. Chem.*, **47**, 1337, (1975).

41. N.F. Atta, A. Galal, A.E. Karagozler, H. Zimmer, J. F. Rubinson and H.B. Mark Jr., *J. Chem. Soc. Chem. Commun.*, **19**, 1347 (1990).